

Technica report n. 384/2019/ENG

**EXPERIMENTAL ASSESSMENT
OF THE GAS PERMEABILITY
OF ENGINEERED BARRIERS IN
A DEEP GEOLOGICAL
REPOSITORY – FINAL REPORT**

Authors: Jiří Svoboda
et al.

CTU in Prague
Prague, May 2019



SÚRAO

Project name: Research support for the safety assessment of a deep geological repository

Subproject Name: *Experimental assessment of the gas permeability of engineered barriers in a deep geological repository*

Report name: *Experimental assessment of the gas permeability of engineered barriers in a deep geological repository – Final Report*

Final report

Client registration number: SÚRAO TZ 384/2019/ENG

Contractor registration number: PB-2019-ZZ-S3831-036-Plynopropustnost_ENG

Investigating institution:

Czech Technical University (CTU – ČVUT)¹

Authors: Jiří Svoboda¹, Radek Vašíček¹, Jiří Štástka¹, Danuše Nádherná¹, Dana Pacovská¹, Jaroslav Pacovský¹

Approval				
Position	Institution	Name	Date	Signature
Technical coordinator (contractor)	ČVUT	Ing. Jiří Svoboda, Ph.D.		
Project manager (contractor)	ÚJV Řež, a. s.	RNDr. Václava Havlová, Ph.D.		
Technical coordinator	SÚRAO	Ing. Jan Smutek, Ph.D.		
Main coordinator	SÚRAO	Ing. Antonín Vokál, CSc.		



SÚRAO



SÚRAO

Contents

1	Introduction	11
2	Gas permeability of bentonite with natural water content	13
2.1	Testing procedure	13
2.2	Assessment	15
2.3	Results.....	17
3	Gas permeability of saturated bentonite.....	22
3.1	Testing procedure	23
3.2	Assessment	26
3.3	Tests conducted.....	27
3.3.1	Homogeneous samples.....	27
3.3.2	Samples with discontinuities.....	28
3.4	Evaluation of the results	41
4	Conclusion	52
5	Literature	54

List of tables:

Tab. 1 Gas permeability test results for the samples with natural water content	19
Tab. 2 Gas permeability test results for the samples with increased water content.....	19
Tab. 3 Results of the breakthrough tests on the homogeneous samples	30
Tab. 4 Results of the breakthrough tests on the samples with discontinuities	37

List of figures:

Fig. 1 Scheme of the apparatus used for the measurement of gas permeability	14
Fig. 2 Example of a test.....	15
Fig. 3 Test PN008	16
Fig. 3 Gas permeability results for the samples with natural water content	17
Fig. 4 – Gas permeability results dependent on water content.....	18
Fig. 5 Gas permeability depending on the available pore space (the ρ_d of the sample is provided for each point in the graph).....	20
Fig. 6 Comparison of the effective gas permeability of BaM with that of B75 (the ρ_d of the sample is given for each point)	20
Fig. 7 Gas permeability results for the samples with increased water content	21
Fig. 9 Scheme of the measurement apparatus	23
Fig. 10 Permeability chamber showing the coupling at the sample inlet for connection to the pressurising system.....	24
Fig. 11 Example of the progress of a pressure test.....	25
Fig. 12 Sample still fitted with permeable plates following removal from its experimental ring	26
Fig. 13 Characteristic progress of the tests.....	27
Fig. 14 Sample P588 (summary)	32
Fig. 15 Sample P589 (summary)	33
Fig. 16 Sample P590 (summary)	34
Fig. 17 Sample P596 (summary)	35
Fig. 18 Sample P624 (summary)	36
Fig. 19 Sample P602 (summary)	38
Fig. 20 Sample P592 (summary)	39
Fig. 21 Sample P597 (summary)	40
Fig. 22 Time to breakthrough for the homogeneous samples (the longer the time, the better the result; the number in the legend indicates the loading cycle)	41
Fig. 23 Pressure drop for the first day for the homogeneous samples (the lower the value, the better the result; the number in the legend indicates the loading cycle)	42

Fig. 24 Swelling pressure at the end of the saturation phase for the homogeneous samples (the higher the value, the better the result; the number in the legend indicates the loading cycle)	43
Fig. 25 Hydraulic conductivity at the end of the saturation phase for the homogeneous samples (the lower the value, the better the result; the number in the legend indicates the loading cycle)	43
Fig. 26 Time to breakthrough for the non-homogeneous samples (the higher the value, the better the result; the number in the legend indicates the loading cycle)	44
Fig. 27 Decrease in pressure for the first day for the inhomogeneous samples (the lower the value, the better the result; the number in the legend indicates the loading cycle)	45
Fig. 28 Swelling pressure at the end of the saturation phase for the non-homogeneous samples (the higher the value, the better the result; the number in the legend indicates the loading cycle)	46
Fig. 29 Hydraulic conductivity at the end of the saturation phase for the non-homogeneous samples (the lower the value, the better the result; the number in the legend indicates the loading cycle)	46
Fig. 30 Swelling pressure dependent on dry density (the number near the point indicates the loading cycle)	47
Fig. 31 Hydraulic conductivity dependent on dry density (the number near the point indicates the loading cycle)	48
Fig. 32 Breakthrough time (the number near the point indicates the loading cycle)	50
Fig. 33 Pressure drop at day 1 (the number near the point indicates the loading cycle)	51

List of abbreviations:

DGR	Deep geological repository
e	Porosity number defined as the pore volume to grain volume ratio of the material
EBS	Engineered barrier system
RAW	Radioactive waste
SNF	Spent nuclear fuel
Sr	Degree of saturation
WDP	Waste disposal package

Abstract

The aim of the “Experimental assessment of the gas permeability of engineered barriers in a deep geological repository” subproject was to launch, based on a detailed literature review, an experimental programme for the assessment of the gas permeability of the engineered barriers considered for the future Czech deep geological repository.

An initial experimental analysis was performed of the behaviour of gases in the engineered barrier material involving the experimental investigation of bentonite and its self-healing ability. Due to the time-consuming nature of such research and the deadline set for the completion of the project, the experimental analysis focused on phenomena associated with the mechanical damage of the bentonite caused by gas pressure. The aim was to commence experimental work based on an initial evaluation of the mechanical influence of gas flow/breakthrough events on the engineered barrier material.

The study was divided into two main areas:

- a. The gas permeability of bentonite with natural water content
- b. Gas breakthrough in saturated bentonite


In view of the time-consuming nature of the study of the dilatant path formation mechanism (which takes months or even years) via the classical method involving a gradual increase in pressure and the determination of the pressure required to obtain breakthrough, an alternative high-pressure gas injection method was chosen for the second area of the study comprising the measurement of the time required to achieve breakthrough as a relative indication of changes between cycles.

In accordance with SÚRAO requirements, so-called BaM bentonite material was subjected to gas permeability research. BaM is an industrially-processed (dried and crushed) Ca-Mg bentonite mixture (it originates from several deposits owned by the Keramost a.s. bentonite processing company).

The results of both areas of the study clearly revealed that the main determinant of the behaviour of BaM material in terms of gas permeability consists of its dry density, i.e. the properties of BaM improve as the dry density increases.

The results obtained from the gas breakthrough tests did not indicate that cyclical gas breakthrough events degrade the material. Whereas in some cases a deterioration in properties was evident, the changes eventually stabilised and were not significant. Conversely, the hydraulic conductivity and swelling pressure values were, in most cases, systematically better than the reference values.

The results revealed the significant influence of time, i.e. long-term saturation exerted a significant impact on the properties of the BaM material. This was particularly evident for the samples with discontinuities. Although the permeability and swelling pressure values did not vary significantly over time, the process of the stabilisation of the breakthrough values lasted significantly longer than it did for the homogeneous samples and, moreover, the behaviour of the material under test conditions differed.

 SÚRAO	<i>Experimental assessment of the gas permeability of engineered barriers in a deep geological repository – final report</i>	Evidenční označení:
		SÚRAO TZ 384/2019/ENG

The gas permeability tests conducted as part of this project were of a pilot character. The breakthrough tests revealed the non-deterministic behaviour of the material and the significant need for the conducting of long-term tests. Whereas the testing of the non-homogeneous material addressed only a simple longitudinal discontinuity, under real conditions, the engineered barrier will feature an extensive network of such discontinuities. Therefore, the gradual upscaling of the issue is required involving the conducting of complex tests. Moreover, the experimental analysis did not address materials that are inhomogeneous due to their form (i.e. pellets), the behaviour of which will also have to be verified in the future.

Keywords

Repository, gas, EBS, swelling, permeability, gas breakthrough

1 Introduction


This report was prepared as part of the SÚRAO “Research support for the safety assessment of a deep geological repository” project which forms an important part of the preparation phase for the construction of the Czech deep geological repository for radioactive waste (hereinafter DGR). The aim of the project is to obtain the data, models, arguments and other information required so as to be able to evaluate potential sites for the location of the repository in terms of long-term safety. Following the conducting of a public procurement procedure, a four-year contract was signed in July 2014 with ÚJV Řež, a.s. and its subcontractors: the Czech Geological Survey; the Czech Technical University in Prague; the Technical University of Liberec; the Institute of Geonics of the Czech Academy of Sciences, v.v.i.; SG Geotechnika a.s.; Progeo, s.r.o.; Chemcomex, a.s. and Research Centre Řež s.r.o. concerning the provision of research support for long-term safety assessment purposes in the following areas:

- i. The behaviour of spent fuel and radioactive waste which cannot be accepted for near-surface storage/disposal in an underground repository environment;
- ii. The behaviour of storage casks for spent fuel and radioactive waste in an underground repository environment;
- iii. The behaviour of damping, filling and other construction materials in an underground repository environment;
- iv. The final design of the disposal wells and their influence on the properties of the surrounding geological environment;
- v. The behaviour of the rock mass;
- vi. The transport of radionuclides from the repository;
- vii. Other characteristics of the sites which might potentially affect the safety of the repository

The aim of this *Experimental assessment of the gas permeability of engineered barriers in a deep geological repository* subproject is to initiate an experimental programme on the gas permeability assessment of the engineered barriers considered for the future Czech deep geological repository based on a detailed literature search.

The objective of this report is to summarise the results of the fourth stage, i.e. the conducting of the initial experimental analysis of the engineered barrier material from the point of view of gas permeability involving the experimental investigation of bentonite and its self-healing ability. Due to the time-consuming nature of such research and the deadline set for the completion of the project, the experimental analysis focused on phenomena associated with mechanical damage to the bentonite caused by gas pressure. The aim was to commence experimental work based on an initial evaluation of the mechanical influence of gas flow/breakthrough events on the engineered barrier material.


In view of the time-consuming nature of the study of the dilatant path formation mechanism (which takes months or even years) via the classical method involving a gradual increase in pressure and the determination of the pressure required to obtain breakthrough, an alternative high-pressure gas injection method was chosen for the second area of the study comprising the measurement of the time required to achieve breakthrough as a relative indication of changes between cycles.

 SÚRAO	<i>Experimental assessment of the gas permeability of engineered barriers in a deep geological repository – final report</i>	Evidenční označení:
		SÚRAO TZ 384/2019/ENG

The study was divided into two main areas:

- a. Gas permeability of bentonite with natural water content
- b. Gas breakthrough in saturated bentonite

In accordance with SÚRAO requirements, so-called BaM bentonite material was subjected to gas permeability research. BaM is an industrially-processed (dried and crushed) Ca-Mg bentonite mixture (it originates from several deposits owned by the Keramost a.s. bentonite processing company).

 SÚRAO	<i>Experimental assessment of the gas permeability of engineered barriers in a deep geological repository – final report</i>	Evidenční označení:
		SÚRAO TZ 384/2019/ENG

2 Gas permeability of bentonite with natural water content

If gas is created in the DGR prior to the saturation of the sealing layer with water, the gas permeability of the engineered barrier material in the initial state, i.e. dry or naturally moist material will be important in terms of the transport of gases. Therefore, the gas permeability of the bentonite material was experimentally assessed with respect to the first part of this phase in the naturally moist state (i.e. in a state consistent with the conditions assumed during the installation of the material in the repository). Part of the assessment consisted of the determination of the dependence of gas permeability on the bulk density of the material.

In accordance with the requirements of the sub-report and the work specification and schedule document, the conducting of a total of 5 tests was planned on bentonite samples with a natural water content. Moreover, in order to determine the dependence of gas permeability on bulk density, samples with a dry density of 1000, 1200, 1400, 1600 and 1800 kg/m³ were produced. It was assumed that the same samples would be further utilised for the subsequent gas pressure testing of the saturated bentonite. However, in order to accelerate the testing process, it was decided to create another set of samples for these tests so that the two test series could be performed in parallel. Following the testing of the gas permeability of the samples with a natural water content, these samples were disassembled to allow for the determination of their moisture content and bulk density. This approach allowed for the better interpretation of the results.

At the request of the Client, the planned gas permeability tests were expanded by the testing of samples with a higher water content. These samples were prepared via the same procedure (compression) as were the samples with a natural water content; however, the initial powder material was pre-wetted, mixed and homogenised for several days prior to compression. The target dry density was the same for these samples, namely 1600 kg/m³. The aim of the tests was to determine the influence of the water content of the samples on gas permeability.

A total of 11 tests was performed (as opposed to the five originally planned tests), including 7 tests on samples with a natural water content and 4 tests on samples with a higher water content. All the tests involved the gradual increase and subsequent reduction in the gas pressure and flow rate. The tests were carried out according to internal procedure no. 182/28 (The Determination of the Gas Permeability of Unsaturated Soils) which is described later in this chapter.

2.1 Testing procedure

An air pressure gas testing apparatus was used to determine gas permeability (Fig. 1). The equipment included a steel cell (chamber) into which the sample was placed. The cell, made exclusively of stainless steel, was fitted with steel flanges connected by means of threaded rods so as to provide for the rigid fixing of the sample placed in the steel ring. The 30 mm diameter cylindrical sample was surrounded on both sides by sintered steel permeable plates in order to prevent the leaching of the material. A piston and a pressure sensor for the

measurement of the swelling pressure of the bentonite were positioned between the upper flange of the chamber and the upper surface of the sample (the sensor was omitted when performing the gas permeability tests on the dry material samples).

The chamber was connected via an inlet to the pressurising system which included a dry air cylinder (max. pressure 230 bar), a regulator for the control of the air injection pressure, a digital pressure gauge (Keller LEO Record, range 0-300 bar) for the recording of the injection pressure at the inlet and a draining valve. The digital pressure gauge, which also included a temperature sensor, stored the measured data in its internal memory at set time intervals. A Bronkhorst MV-104 flowmeter with a measuring range of 0-20 standard litres per minute (Nl/min) was connected to the output of the sample. The continuous recording of information from the flowmeter was provided for via control software installed on a computer connected to the system.

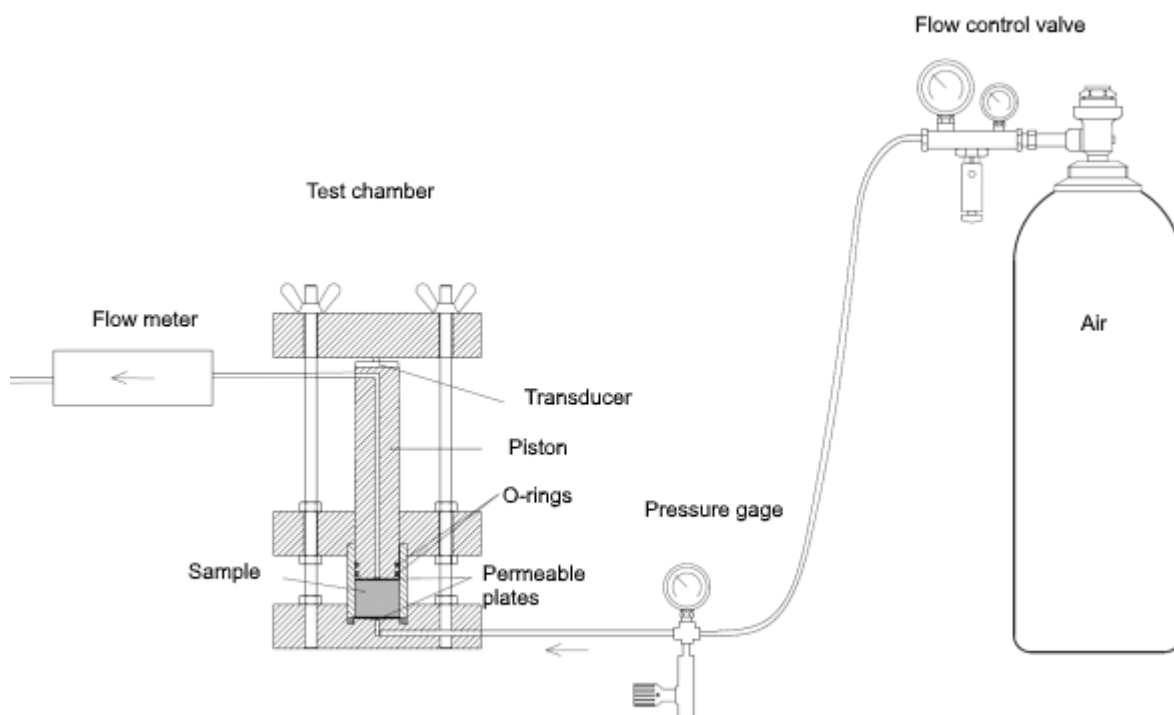


Fig. 1 Scheme of the apparatus used for the measurement of gas permeability

The first stage of the testing procedure consisted of the pressing of the samples directly into the rings so as to prevent the formation of joints between the sample and the ring. The amount of material was determined depending on the required bulk density and the volume of the sample. The diameter and height of all the samples for the purposes of this sub-report were 30 mm and 20 mm respectively. The exact height and weight of the samples were determined via measurement/weighing following the completion of the preparation of the samples. The initial water content was determined via the gravimetric method using the same material as that used for the samples.

The next stage consisted of the completion of the experimental cell, its attachment to the experimental apparatus and the commencement of the recording of the data. This was followed by the measurement of gas permeability itself.

With concern to the measurement of gas permeability, the injection pressure was increased incrementally and the flow of gas recorded. An example of a test is shown in Fig. 2. The duration of each increment was selected in such a way that the flow was always stabilised. Following the final increase in injection pressure, the test was either terminated or subjected to incremental reductions in the injection pressure.

Following the completion of each test, the final water content of the sample was determined using the gravimetric method.

GT_74: vzorek SAB_06

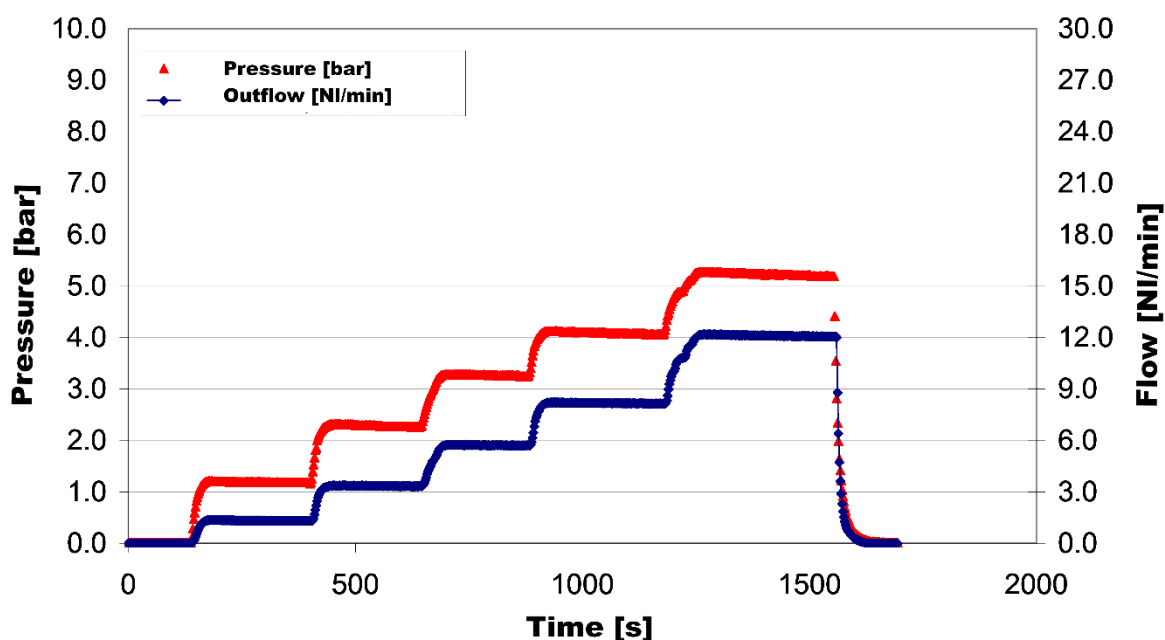


Fig. 2 Example of a test

2.2 Assessment

The test evaluation procedure involved the calculation of the gas permeability for all the pressure levels applied. In order to directly obtain the gas permeability values of the samples, they would have to have been completely dry. However, the drying of the samples in the oven was not possible since it would have caused irreversible damage to their microstructures. Therefore, since the test samples were not completely dry, the value was obtained in the form of the effective gas permeability (k_{ef}), which corresponds to the product of the theoretical absolute permeability determined via the measurement of the gas (intrinsic gas permeability - k_{ig}) and the relative gas permeability (k_{rg}), which expresses the degree of saturation of the sample by the gas (accorded values of from 0 to 1). The effective gas permeability was calculated using equation (1) that expresses Darcy's law for compressible fluids.

$$k_{ef} = k_{ig} \cdot k_{rg} = \frac{2Q \cdot \mu_g \cdot L \cdot P_0}{A \cdot (P_1^2 - P_2^2)} \quad (1)$$

Where:

- k_{ef} Effective gas permeability [m²]
- k_{ig} Intrinsic gas permeability [m²]
- k_{rg} Relative gas permeability [-]
- Q Flow [m³s⁻¹]
- μ_g Dynamic viscosity [Pa.s]
- L Sample height [m]
- A Sample area [m²]
- P_0 Reference (atmospheric) pressure [Pa]
- P_1 Sample inlet pressure [Pa]
- P_2 Sample outlet pressure (atmospheric) [Pa]

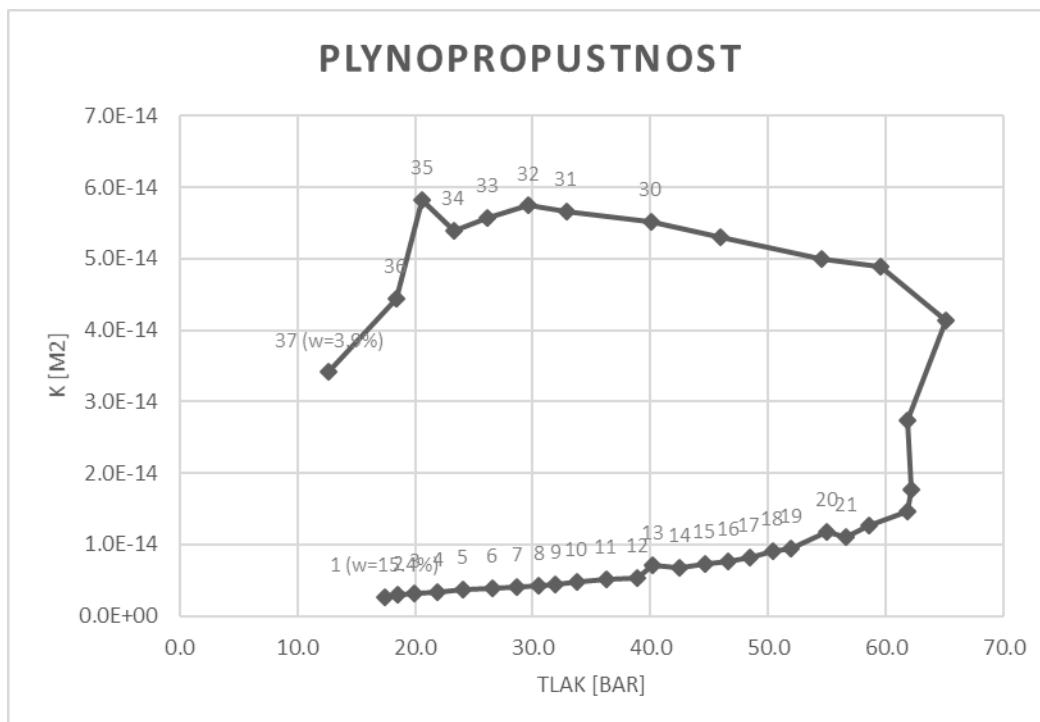


Fig. 3 Test PN008

Fig. 3 illustrates the typical progress of a pressure test. The graph plots the injection pressure curve and the resulting gas permeability calculated from the flow of gas through the sample. The test commenced with the injection of low pressure air (the point marked 1 with the initial water content); the injection pressure was then gradually increased and the flow recorded (other points on the curve - the number indicates the reading sequence). After reaching a

maximum pressure of ~65 bar (point no. 25), the process was reversed, i.e. the pressure was gradually reduced. The recording of the pressure and flow values continued up to the conclusion of the test (point 37). The final water content of the sample was then determined.

2.3 Results

The results of the tests on the samples with natural water content are provided in Tab. 1 and Fig. 4 (note - the regression equation shown in Fig. 4 does not include the first, i.e. outlier measurement). The basic characteristics of each of the samples are presented along with the typical effective permeability (the value that best approaches the trend – generally corresponding to the maximum pressure level). The values at the start of the test (first pressure stage) and the end of the test (final pressure stage) are also provided.

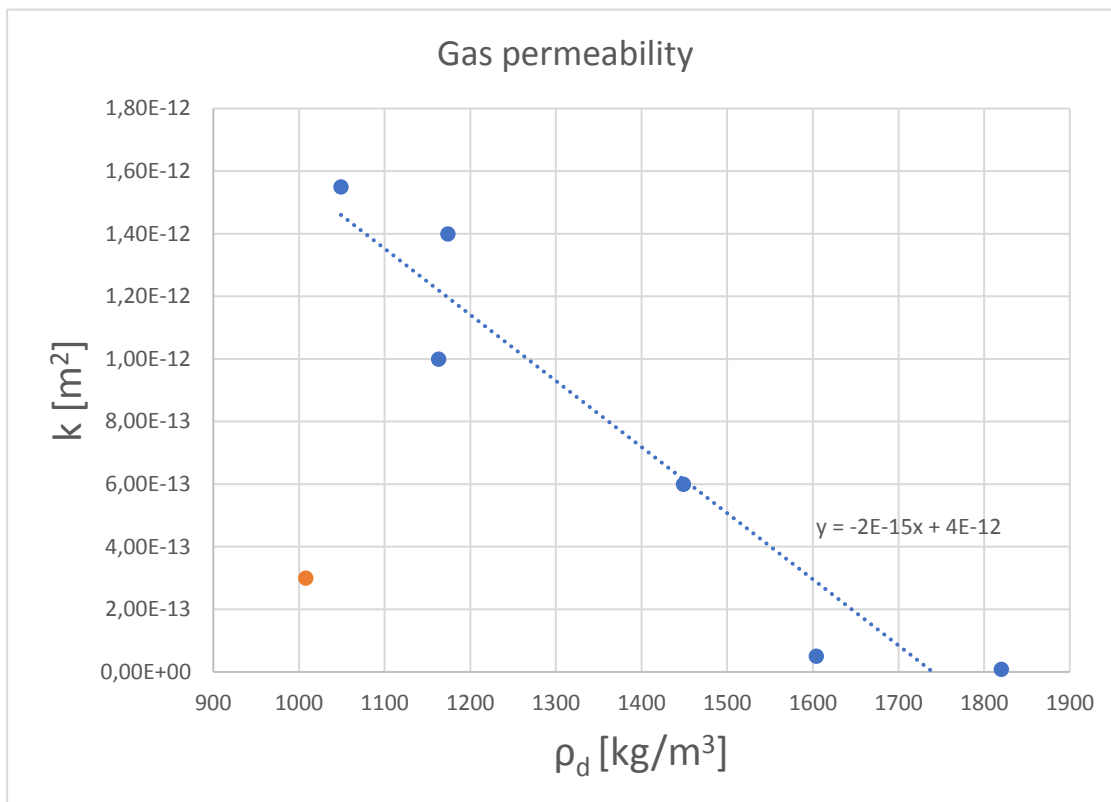


Fig. 4 Gas permeability results for the samples with natural water content

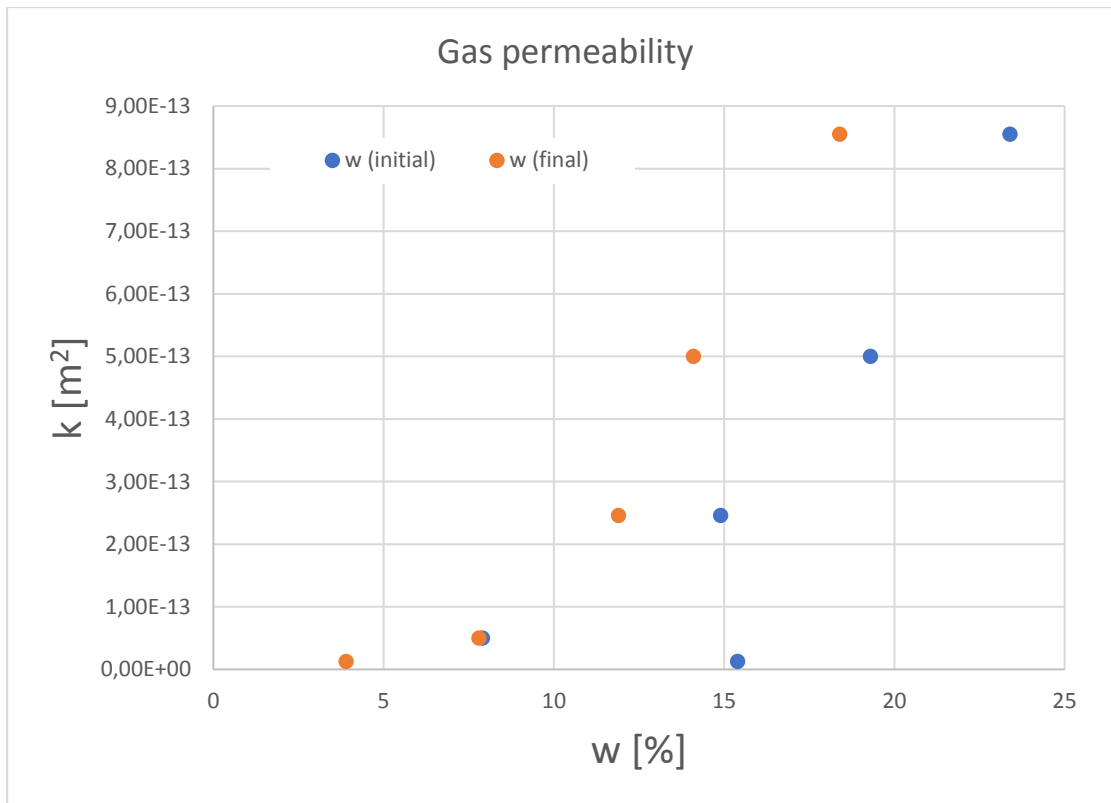


Fig. 5 – Gas permeability results dependent on water content

The results reveal a clear dependence between dry density and gas permeability, which was due to the decrease in the available pore space (Fig. 6 and Fig. 7). Higher bulk densities reflect a higher content of solids in the same volume and, therefore, less available free space.

The test results for the samples with increased water contents are shown in Tab. 2, Fig. 5 and Fig. 8. The results are shown including the accepted results from the samples with natural water content. All the samples were prepared with a reference target dry density of 1600 kg/m³ and varying amounts of water.

The results shown in Fig. 5 appear to indicate that the gas permeability increased with increasing water content. However, this apparent dependence is deceptive since the trend was, in fact, due to the differing bulk densities of the samples (Fig. 8), concerning which even a small change in the bulk density exerted a significantly greater influence on permeability than did the change in the water content. Moreover, it is evident from the test results that permeability increased with the drying of the samples (Fig. 3).

Tab. 1 Gas permeability test results for the samples with natural water content

						at the start of the test					after / at the end of the test				
sample	sample height	ρ_d	n	e	k_{ef}	ρ	w	Sr	e(1-Sr)	k_{ef}	ρ	w	Sr	e(1-Sr)	k_{ef}
no.	mm	kg/m ³	(porosity)	(porosity no.)	m ²	kg/m ³	%	(degree of saturation)	(pores available)	m ²	kg/m ³	%	(degree of saturation)	(pores available)	m ²
PN015	20	1008	0.627	1.679	3.00E-13	1096	8.7	0.14	1.443	3.86E-14	996	2.3	0.04	1.616	2.96E-13
PN017	19.2	1049	0.611	1.574	1.55E-12	1142	8.9	0.15	1.333	1.48E-13	1068	2.8	0.05	1.498	2.49E-13
PN001	17.2	1174	0.565	1.300	1.40E-12	1267	7.9	0.16	1.086	1.16E-12	---	3.2	0.07	1.213	2.00E-12
PN002	20.5	1163	0.569	1.322	1.00E-12	1255	7.9	0.16	1.108	1.86E-12	---	4.6	0.09	1.197	2.09E-12
PN003	20.3	1449	0.463	0.863	6.00E-13	1564	7.9	0.25	0.650	9.00E-13	1492	5.1	0.16	0.725	1.49E-12
PN004	20.8	1604	0.406	0.683	5.00E-14	1732	7.9	0.31	0.470	5.21E-14	1707	7.8	0.31	0.472	5.93E-14
PN005	20.5	1820	0.326	0.484	9.00E-15	1964	7.9	0.44	0.270	1.07E-14	1938	8.4	0.47	0.256	9.10E-15

Tab. 2 Gas permeability test results for the samples with increased water content

						at the start of the test					after / at the end of the test				
sample	sample height	ρ_d	n	e	k_{ef}	ρ	w	Sr	e(1-Sr)	k_{ef}	ρ	w	Sr	e(1-Sr)	k_{ef}
PN007	21.8	1545	0.428	0.748	8.55E-13	1906	23.4	0.85	0.115	3.45E-14	1846	18.4	0.67	0.250	2.42E-13
PN008	20.2	1698	0.371	0.590	1.26E-14	1960	15.4	0.71	0.173	2.65E-15	1772	3.9	0.18	0.485	3.41E-14
PN013	19.8	1520	0.437	0.776	5.00E-13	1813	19.3	0.67	0.254	9.45E-15	1761	14.1	0.49	0.395	4.66E-13
PN016	20.3	1602	0.407	0.685	2.46E-13	1840	14.9	0.59	0.282	2.36E-14	1786	11.9	0.47	0.363	9.21E-14
PN004	20.8	1604	0.406	0.683	5.00E-14	1732	7.9	0.31	0.470	5.21E-14	1707	7.8	0.31	0.472	5.93E-14

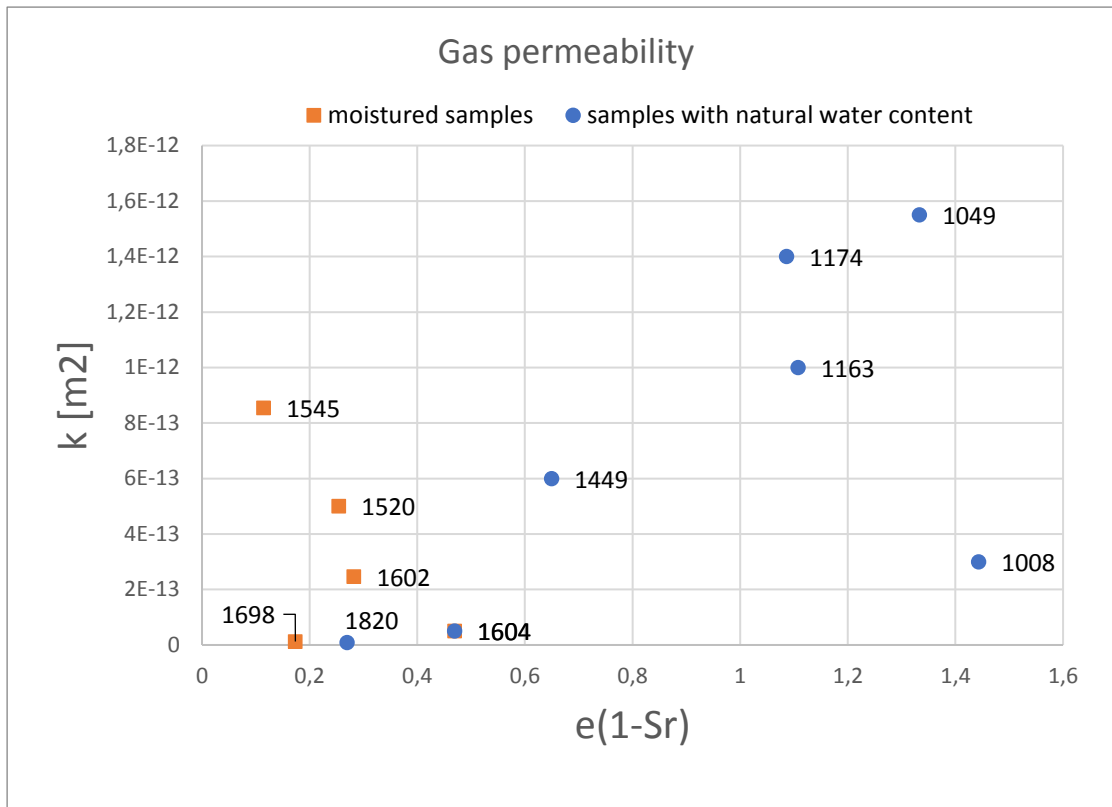


Fig. 6 Gas permeability depending on the available pore space (the p_d of the sample is provided for each point in the graph)

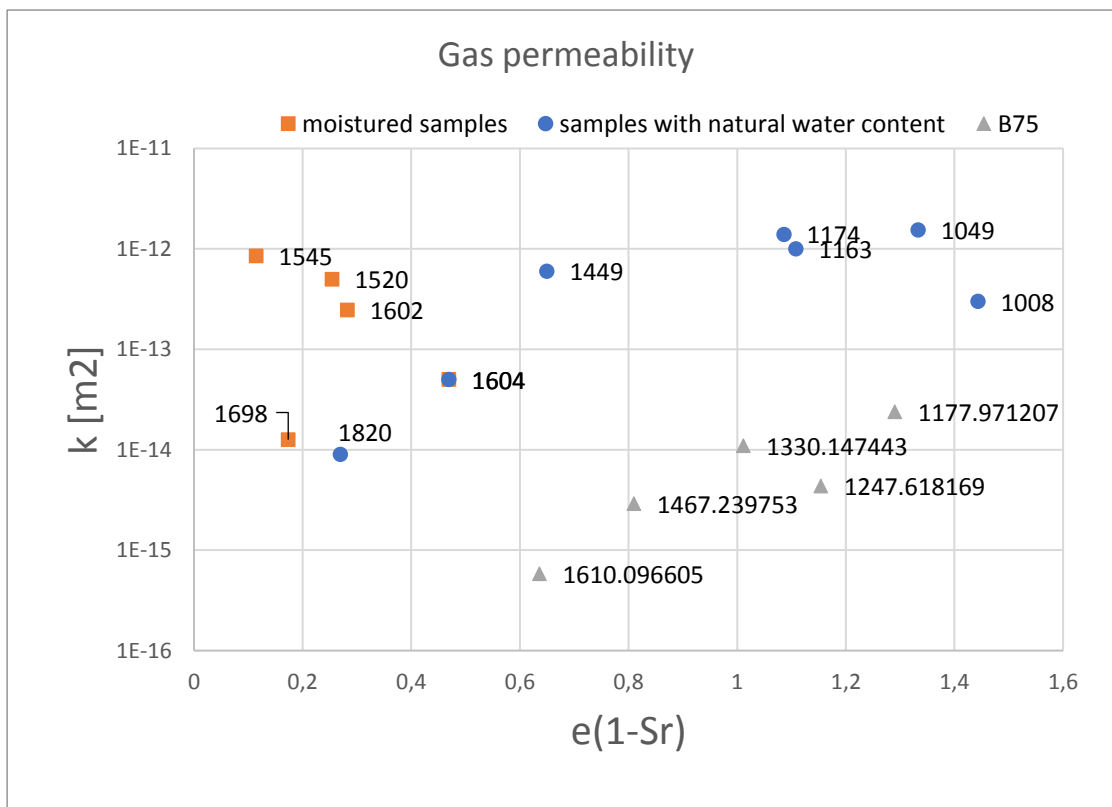


Fig. 7 Comparison of the effective gas permeability of BaM with that of B75 (the p_d of the sample is given for each point)

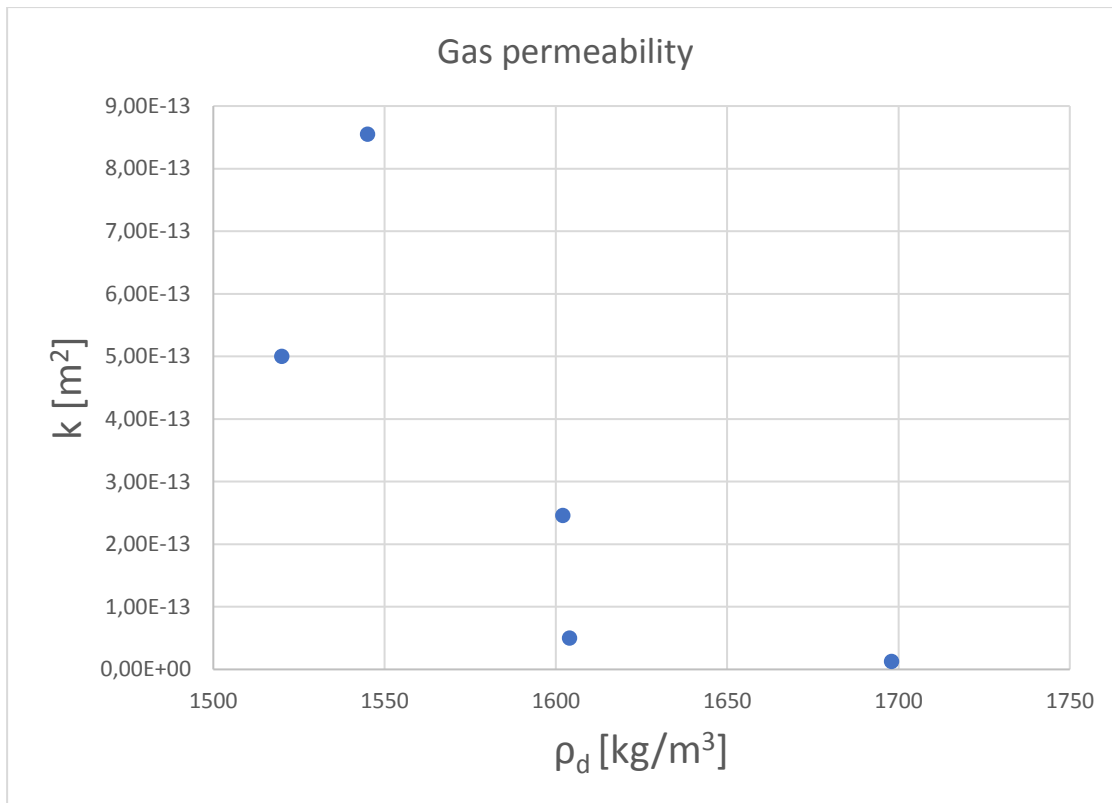


Fig. 8 Gas permeability results for the samples with increased water content

3 Gas permeability of saturated bentonite

An increase in pressure caused by gas created in the DGR might, in extreme cases, lead to mechanical damage to the sealing barrier surrounding the disposed of waste. Such breaches (breakthrough) will occur once the pressure of the created and accumulating gas exceeds the total stress within the sealing barrier. Depending on the gas pressure and the bentonite swelling pressure ratio, this phenomenon may lead to the immediate or long-term creation of preferential paths. As soon as a preferential route is created, the gas will gradually escape thus leading to a decrease in pressure. One of the most important issues in terms of repository safety lies in the dynamics of the development of such events and, in particular, the post-event situation, i.e. whether the sealing barrier will be able to reconsolidate via the bentonite self-healing process and thus continue to fulfil its function.

The research in this stage of the project focused on the study of the dynamics of mechanical damage caused by gas and its influence on the material that makes up the sealing layer of the engineered barrier system. The research continued with the loading of saturated bentonite samples with air at high pressures (~12 MPa). The experimental investigation concerned the breakthrough dynamics of the material dependent on the swelling pressure (bulk density) and, in particular, the occurrence of self-healing and whether the sealing ability of the material deteriorates following the repetition of material stress (increased permeability, reduction in the breakthrough time).

In accordance with the subproject requirements and the work specification and schedule document, it was decided that a total of 3 saturation-breakdown test cycles would be conducted on bentonite samples with dry densities of 1400, 1600, 1800 kg/m³, both for homogeneous samples and samples featuring discontinuities.

The homogenous samples were prepared via the pressing of bentonite powder directly into the experimental cells. The discontinuity samples were prepared in a similar way to the homogeneous samples; however, they were removed from the cells following pressing and a cut was inserted along their height (parallel to the direction of flow); they were then returned to the moulds. Unfortunately, this process always involves the loss of a certain amount of material and, therefore, it is difficult to accurately determine the resulting bulk density.

Each sample was subjected to cyclical testing involving the initial saturation of the samples (and the determination of the hydraulic conductivity and swelling pressure) followed by gas testing up to the breakthrough of the samples. The tests were conducted according to internal procedures 182/21 (The Determination of Hydraulic Conductivity and Swelling Pressure, which complies with ČSN CEN ISO/TS 17892-11) and 182/29 (The Determination of the Time Required to Achieve Gas Pressure Breakthrough in Saturated Bentonite).

3.1 Testing procedure

The apparatus illustrated in Fig. 9 was used to perform the gas pressure tests. The set-up included a steel cell (chamber) containing the material sample. The cell forms a part of a permeability meter used by the CEG for the measurement of the swelling pressure and hydraulic conductivity of bentonite (CEG internal procedure nos. 182/21 and 182/22, which complies with ČSN CEN ISO / TS 17892-11). Part of the cell, made exclusively of stainless steel, was fitted with steel flanges connected by means of threaded rods so as to provide for the rigid fixing of the sample placed in the steel ring. The top and bottom of the 30 mm diameter cylindrical sample were fitted with sintered steel permeable plates in order to prevent the leaching of the material. A piston and a pressure sensor for the measurement of the swelling pressure of the bentonite were positioned between the upper flange of the chamber and the upper surface of the sample. The pressure sensor was connected to the central data logger.

The permeability chamber Fig. 10 was connected via an inlet to the pressurising system which included a dry air cylinder (max. pressure 230 bar, volume 2.0 l), a filling and draining valve and a digital pressure gauge (Keller LEO Record, range 0-300 bar) for the recording of the injection pressure at the inlet. The digital pressure gauge, which also included a temperature sensor, stored the measured data in its internal memory at set time intervals.

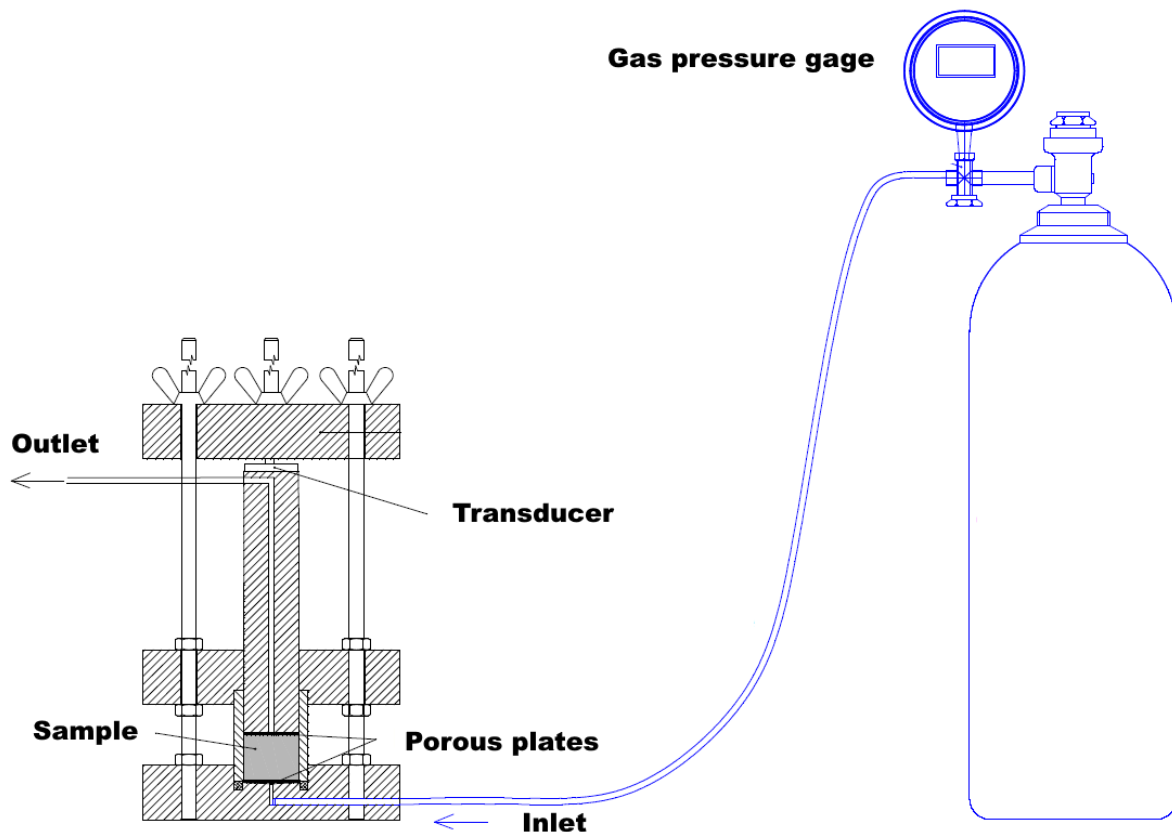


Fig. 9 Scheme of the measurement apparatus



Fig. 10 Permeability chamber showing the coupling at the sample inlet for connection to the pressurising system

The principle of the test procedure was to load the sample with constant air pressure and to measure the time required to attain breakthrough. Thus, the test did not serve to determine the breakthrough pressure as do tests involving linear or incremental increases in gas pressure at the inlet to the sample. The test procedure allowed for the monitoring of the injection pressure at the inlet to the sample and the total sample stress as measured by the pressure sensor on the piston (i.e. the swelling pressure that is influenced by the injection pressure).

The selected inlet air pressure value was above the swelling pressure limit value determined in the saturation phase. The swelling pressure of the bentonite is dependent on the bulk density of the sample; e.g. for the B75 material often tested by the CEG, the swelling pressure for dry densities ranging from 1.25 to 1.60 Mg/m³ varies between 1 and 8 MPa. The maximum working pressure of the pressurising system was 23 MPa.

The first stage of the test procedure consisted of the preparation of the samples which were pressed directly into the experimental rings. The samples with discontinuities were removed from the cell, incised longitudinally and then returned to the cell. The amount of material was determined depending on the required bulk density and the volume of the sample. According to the requirements of the subproject, the diameter of all the samples was 30 mm with a height of 20 mm.

The exact height and weight were determined via measurement and weighing following the completion of the sample preparation stage. The initial water content was determined during the preparation of the samples via the gravimetric method using the same material.

In order to obtain saturation, the samples were saturated in the first phase in a permeator (CEG internal procedures 182/21 and 22) at a constant inlet water pressure via which the flow of water and the stress on the pressure sensor resulting from the swelling of the bentonite were measured. The samples were considered to be fully saturated once a steady water flow and a

constant stress acting on the pressure sensor were registered. The usual saturation time was from 1 to 3 weeks.

The next stage involved disconnection from the permeator and connection to the apparatus for the testing of the gas permeability of the saturated bentonite. This was followed by the determination of the time required to attain gas pressure breakthrough via the following procedure:

1. Assembly and connection of the pressurising system (as shown in Fig. 9).
2. Switching on of the recording digital pressure gauge located at the sample inlet
3. Conducting of the pressure tests
 - Opening of the cylinder cap and the gradual opening of the filling valve until fully opened
 - Adjustment of the inlet pressure to the prescribed value using the relief valve where necessary
 - During testing, the control recording of the measured pressure values
 - End of the test following breakthrough and the subsequent attainment of the sample inlet pressure
 - Depressurisation of the injection system following the end of the test procedure
4. Download of data from the digital pressure gauge

An example of the progress of a pressure test is shown in Fig. 11. In this case, the sample was loaded with a constant pressure of 120 bar. After attaining breakthrough (3 October 2014 at around 3.50), the inlet pressure fell gradually to zero (complete emptying of the pressure cylinder).

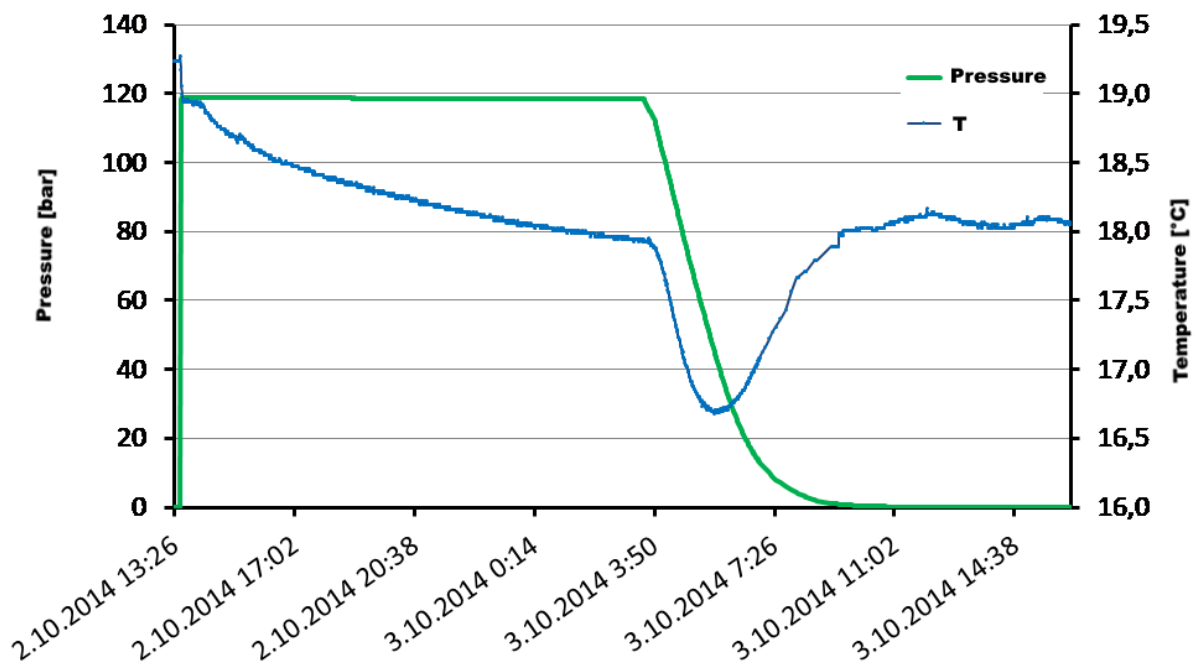


Fig. 11 Example of the progress of a pressure test

Upon completion of the test phase, the chamber was disconnected from the apparatus and reconnected to the permeator in order to repeat the saturation-breakdown cycle or was disassembled.

In the case of the final saturation-breakthrough cycle, the chamber was disassembled and the sample removed from the ring with the assistance of the piston following the end of the test phase. Thus, following the removal of the plates, it was possible to visually check the condition of the surface and substrate of the cylindrical samples. Fig. 12 shows a bentonite sample following the conducting of a gas pressure test; a number of discontinuities can be seen which were caused by the drying of the sample with flowing air and which probably represent original preferential gas flow pathways.

In addition, it was possible to determine the final water content of the sample.

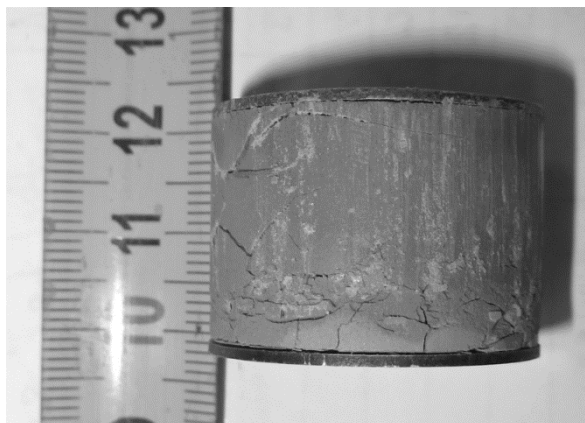


Fig. 12 Sample still fitted with permeable plates following removal from its experimental ring

3.2 Assessment

The main outcomes of the tests consisted of the determination of the time required to attain breakthrough and the provision of interesting information on the progress of pressure with the flow of air through the samples following breakthrough. Fig. 13 shows the characteristic progress of pressure during the conducting of the gas pressure tests.

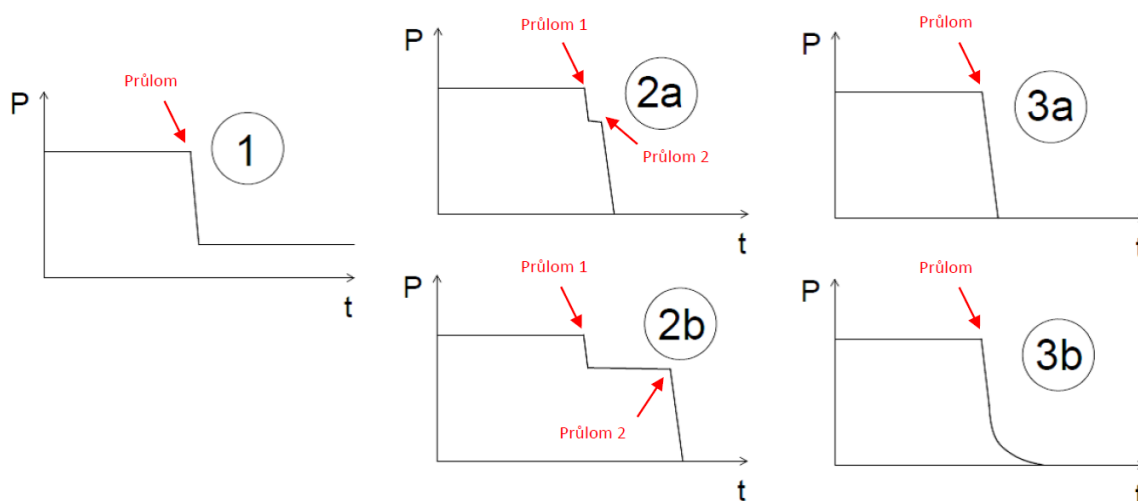


Fig. 13 Characteristic progress of the tests

3.3 Tests conducted


In accordance with the requirements of the sub-report and the work specification and schedule document, it was planned that a total of 2-3 saturation-breakthrough test cycles would be conducted on Černý vrch bentonite samples (both homogeneous and with discontinuities) with dry densities of 1400, 1600 and 1800 kg/m³.

In total (all the samples together) it was planned that 6-9 saturation-breakdown cycles would be conducted for each type of sample. Following a request from the Client, the material was changed from Černý vrch to BaM bentonite.

3.3.1 Homogeneous samples

Work began in August 2017 with the preparation of the first homogeneous samples with target dry densities of 1400 kg/m³ (P589) and 1600 kg/m³ (P590). The sample set was subsequently expanded to include a sample with a target dry density of 1200 kg/m³ (P588), which was originally destined for the verification of the test procedure and which was to be disassembled immediately following the first test; however, due to problems with sample P596 (see below), it was decided to continue the testing of this sample.

In September 2017, a sample with a target dry density of 1800 kg/m³ (P596) was added to the sample series. However, during the testing stage it was found that the swelling pressure of this homogeneous sample was so high that no breakthrough could be attained in the gas pressure test. Therefore, following agreement with the Client, the sample was replaced in February 2018 by a sample with a dry density of 1700 kg/m³ (P624). Due to the limited time available, this sample was subjected to just two saturation-breakdown cycles. A total of four saturation-breakdown cycles were performed on the P588, P589 and P590 samples.

 SÚRAO	<i>Experimental assessment of the gas permeability of engineered barriers in a deep geological repository – final report</i>	Evidenční označení:
		SÚRAO TZ 384/2019/ENG

A total of 15 saturation-breakdown cycles were performed as opposed to the 6-9 originally planned.

An overview of the tests and the results for the homogeneous samples is provided in Tab. 3, while Fig. 14 - Fig. 18 show all the measured values for each of the samples. The figures show a graph that illustrates:

- Total stress measured on the piston at the top of the sample (blue curve).
- An indicative value for hydraulic conductivity (red curve - filtration coefficient). This value is based on the measured flow in the sample. Readings were made at irregular intervals (the aim of the readings was to determine the steady state flow).
- Ambient temperature (yellow curve). Because of the scale used along the Y axis, the values in the graph have been reduced by 15°C (e.g. 5°C in the graph corresponds to a real value of 20°C).
- The progress of injection pressure during the individual pressure breakthrough tests. The curves are distinguished by the PNxxx protocol number.

Furthermore, the graphs for each of the tests are accompanied by descriptions that indicate:

- Swelling pressure before the start of the test procedure
- The time to attain breakthrough or a drop in injection pressure for day 1 for those tests where breakthrough did not occur
- Gas test protocol number
- Swelling pressure after the final test prior to sample disassembly (if measured)

3.3.2 Samples with discontinuities

Work commenced in September 2017 with the preparation of the first samples with target dry densities of 1600 kg/m³ (P592) and 1800 kg/m³ (P597).

The sample preparation procedure was as follows: firstly, the samples were pressed into the experimental rings in a manner identical to that concerning the homogeneous samples (i.e. homogeneous samples of 1600 and 1800 kg/m³). Subsequently, the samples were removed from the ring, a cut was made along their heights and the samples returned to the moulds. The following procedure was identical to that regarding the homogeneous samples. The procedure resulted in a loss of material and thus a lower average bulk density (see Tab. 4). Unfortunately, it was not possible to accurately control the bulk density for these samples.

In November 2017, following the disintegration of a further sample with a planned bulk density of 1400 kg/m³, the test series was supplemented with a sample with a target dry density of 1500 kg/m³ (P605).

Four saturation-breakthrough cycles were performed on sample P592, following which the sample was irrigated by mistake instead of disassembly. Therefore an additional 5th breakthrough test was performed afterwards. Five saturation-breakthrough cycles were performed on samples P597 and P602.

The need to conduct a higher number of saturation-breakthrough tests was due to the behaviour of the samples, i.e. no breakthrough occurred with concern to several of the tests (in contrast to the tests on the homogeneous samples), rather a gradual decrease in the injection pressure was observed. Moreover, a comparison of the results of individual cycles revealed no stabilisation.

It was suspected that the gradual decrease in the injection pressure (e.g. concerning the first tests on samples P597 and P602) was due to the passage of gas along the walls of the experimental cells. Hence, the saturation time was extended for the subsequent cycles. In addition, the experimental apparatus was inspected for possible leaks so as to eliminate the possibility of sealing issues; however, no leaks were discovered.

A total of 15 saturation-breakdown cycles (all the samples together) was performed as opposed to the 6-9 originally planned.

An overview of the tests and the results for the samples with discontinuities is provided in Tab. 4, while Fig. 19 - Fig. 21 show all the measured values for each of the samples. The figures show a graph that illustrates:


- Total stress measured on the piston at the top of the sample (blue curve).
- An indicative value for hydraulic conductivity (red curve - filtration coefficient). This value is based on the measured flow in the sample. Readings were made at irregular intervals (the aim of the readings was to determine the steady state flow).
- Ambient temperature (yellow curve). Because of the scale used along the Y axis, the values in the graph have been reduced by 15°C (e.g. 5°C in the graph corresponds to a real value of 20°C).
- The progress of injection pressure during the individual pressure breakthrough tests. The curves are distinguished by the PNxxx protocol number.

Furthermore, the graphs for each of the tests are accompanied by descriptions that indicate:

- Swelling pressure before the start of the test procedure
- The time to attain breakthrough or a drop in injection pressure for day 1 for those tests where breakthrough did not occur
- Gas test protocol number
- Swelling pressure after the final test prior to sample disassembly (if measured)

Tab. 3 Results of the breakthrough tests on the homogeneous samples

Sample no.	Cycle	Target ρ_d	ρ_d	Saturation time	Swelling pressure	Hydraulic conductivity (K)	Breakthrough test no.	Injection pressure	Breakthrough time
		[kg/m ³]	[kg/m ³]	[days]	[MPa]	[m/s]		[bar]	[h]
P588	1	1200	1165	124	0.52	2.90E-12	PN006	139	0.3
	2			85	not possible (gas test prestressed the sample); 7.15/6.53	2.12E-12	PN019	136	6.6
	3			60	not possible (gas test prestressed the sample); 6.77	1.10E-12	PN025	135	5.5
	4			78	not possible (gas test prestressed the sample); 6.87	9.74E-13	PN033	133	1.4
				0	not possible (gas test prestressed the sample); 7.018		after PN033		
P589	1	1400	1396	154	1.1	1.03E-12	PN009	133	19
	2			58	0.86	7.11E-13	PN020	137	29.9
	3			61	0.81	7.68E-13	PN026	134	44.2
	4			87	0.7695	8.65E-13	PN030	133	15.9
P590	1	1600	1522	154	5.41	1.15E-13	PN011	138	19.5
	2			59	3.43	1.94E-13	PN021	139	gradual decline to 137.36 bar for the 1st day
	3			61	3.93	2.96E-13	PN027	136	gradual decline to 53.35 bar for the 1st day
	4			78	3.855	3.27E-13	PN032	125	23.7 h, gradual decline to 31.86 bar for the 1st day
				0	3.62		after PN032		
P596	1	1800	1774	108	17.53	7.82E-14	PN012	136	gradual decline to 6.84 bar for the 1st day
				The sample had a swelling pressure higher than the injection pressure.					

 SÚRAO	<i>Experimental assessment of the gas permeability of engineered barriers in a deep geological repository – final report</i>	Evidenční označení:
		SÚRAO TZ 384/2019/ENG

P624	1	1700	1646	91	10.93	1.38E-13	PN023	135	gradual decline to 41.3 bar for the 1st day
	2			98	11.78	1.72E-13	PN031	132	gradual decline to 3.18 bar for the 1st day, failure 700h
	The sample had a swelling pressure very similar to the injection pressure.								

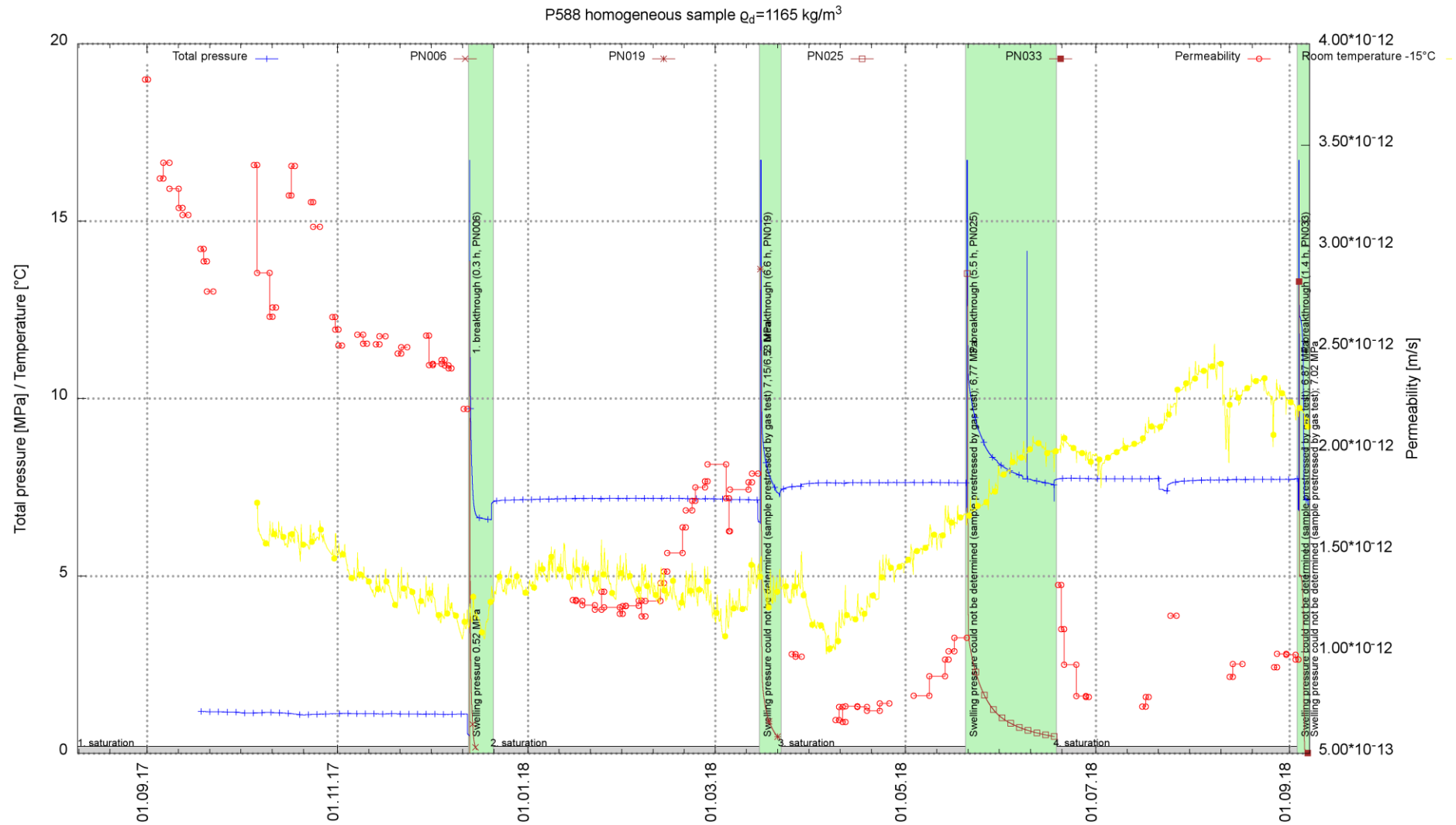


Fig. 14 Sample P588 (summary)

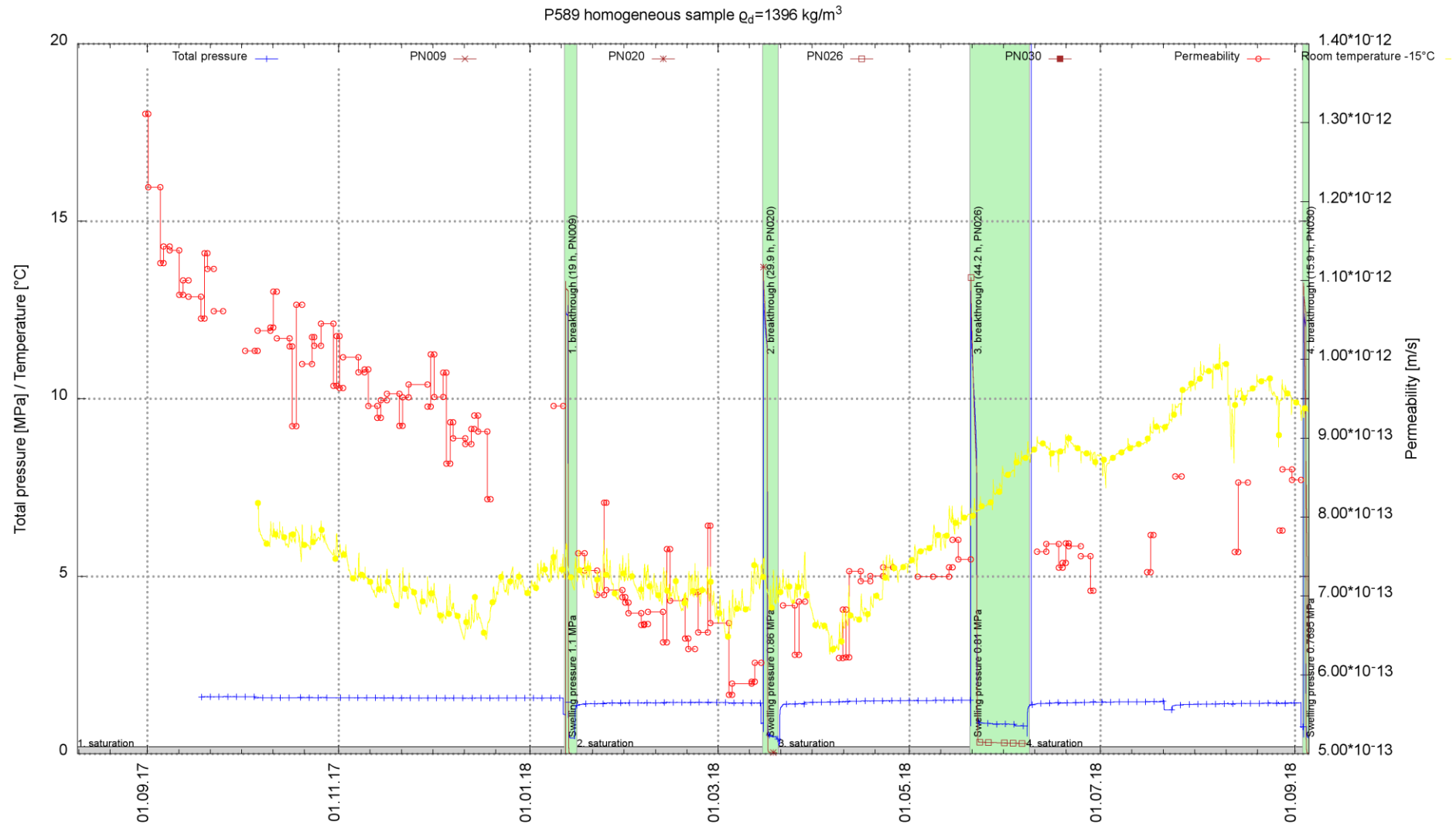


Fig. 15 Sample P589 (summary)

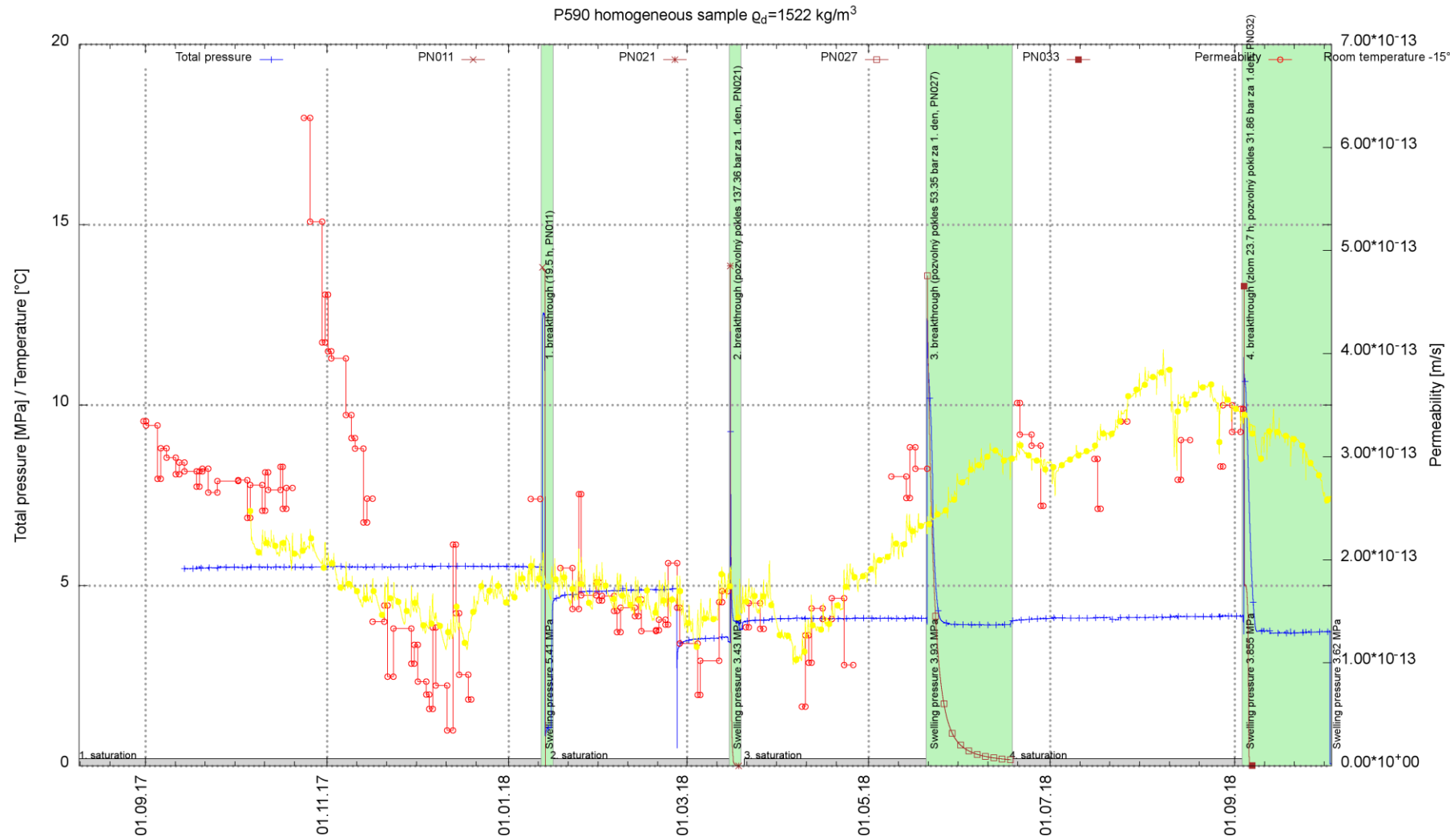


Fig. 16 Sample P590 (summary)

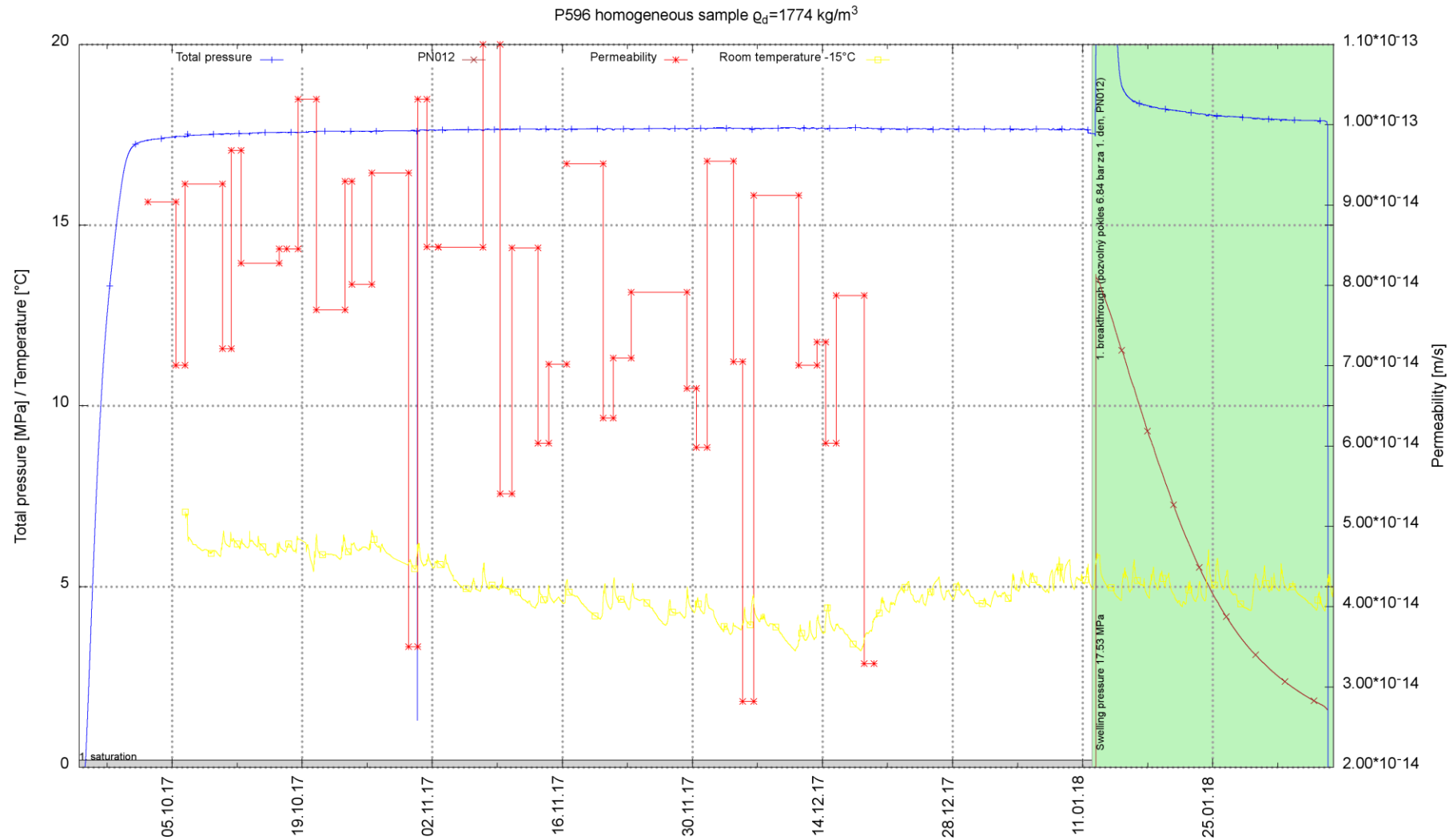


Fig. 17 Sample P596 (summary)

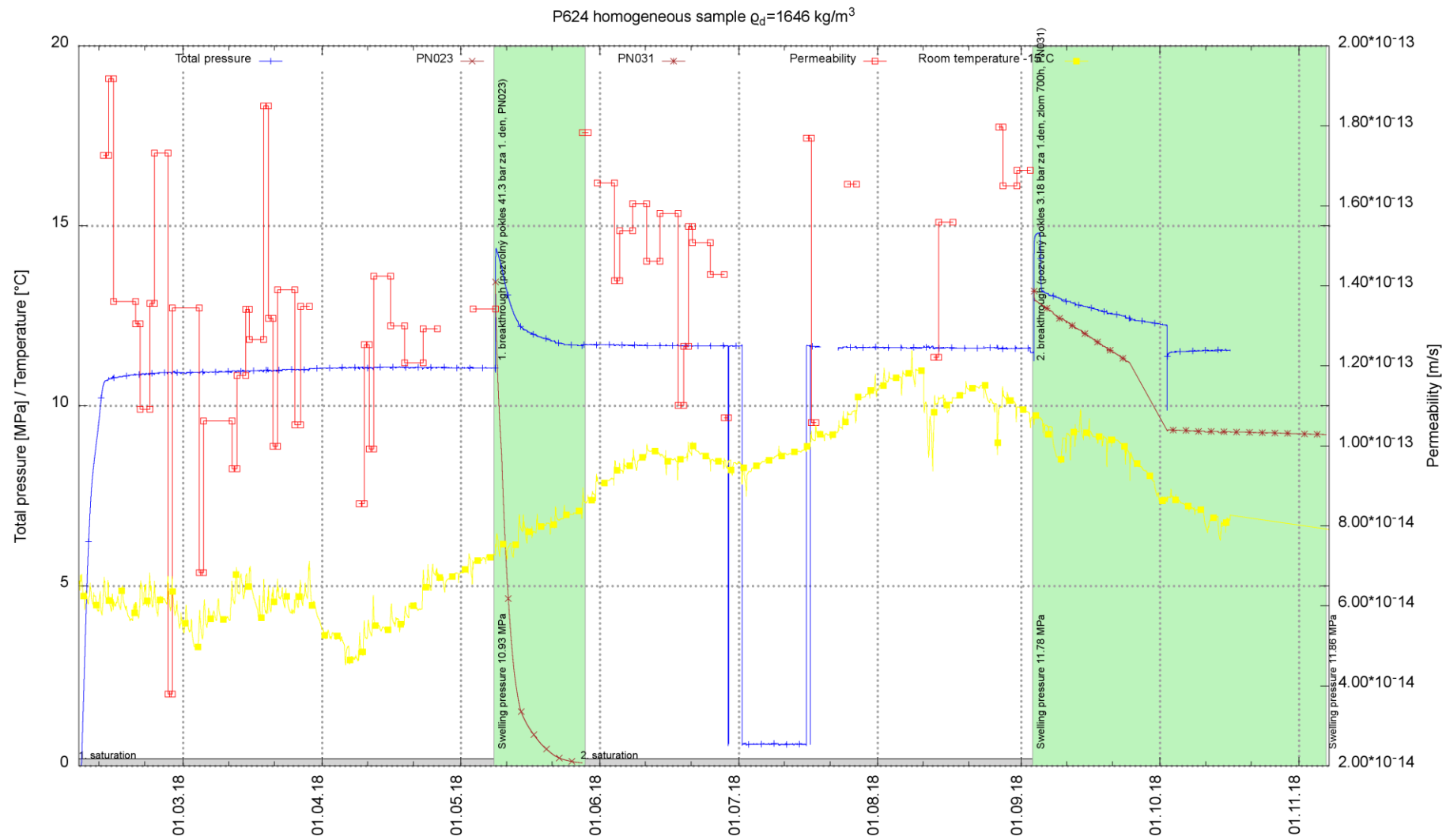


Fig. 18 Sample P624 (summary)

Tab. 4 Results of the breakthrough tests on the samples with discontinuities

Sample no.	Cycle	Target ρ_d (prior to cutting)	ρ_d	Saturation time	Swelling pressure	Hydraulic conductivity (K)	Breakthrough test no.	Injection pressure	Breakthrough time
		[kg/m ³]	[kg/m ³]	[days]	[MPa]	[m/s]		[bar]	[h]
P602	1	1500	1355	116	2.07	4.23E-13	PN018	135	gradual decline to 128.2 bar for the 1st day, duration of decrease 11 h
	2			70	1.9	5.29E-13	PN028	136	1.1
	3			108	1.81	7.00E-13	PN034	136	11.1 (47.23)
	4			65	2.25	7.47E-13	PN038	136	36.3, gradual decline to 58.5 bar for the 1st day
	5			45	1.54	6.34E-13	PN040	136	4.5
					1.65		after PN040		
P592	1	1600	1345	126	1.38	1.08E-12	PN010	134	14.55
	2			52	1.06	4.82E-13	PN022	137	19.2
	3			74	0.93	4.02E-13	PN029	135	21.1 (96.1).
	4			92	0.99	6.00E-13	PN035	134	26.2 (50.4)
	5			0	0.98	N/A	PN037	136	2.4
					0.88		after PN037		
P597	1	1800	1644	112	9.67	1.48E-13	PN014	137	gradual decline, 57.6 bar for the 1st day
	2			110	10.69	1.37E-13	PN024	134	gradual decline, 10.85 bar for the 1st day
	3			130	11.04	1.77E-13	PN036	137	gradual decline to 7.5 bar for the 1st day, potential breakthrough 170.2
	4			49	10.61	1.36E-13	PN039	136	35.4; 36.7
	5			55	9.67	1.34E-13	PN041	126	gradual decline to 10.85 bar for the 1st day and stabilised
					10.51		after PN041		

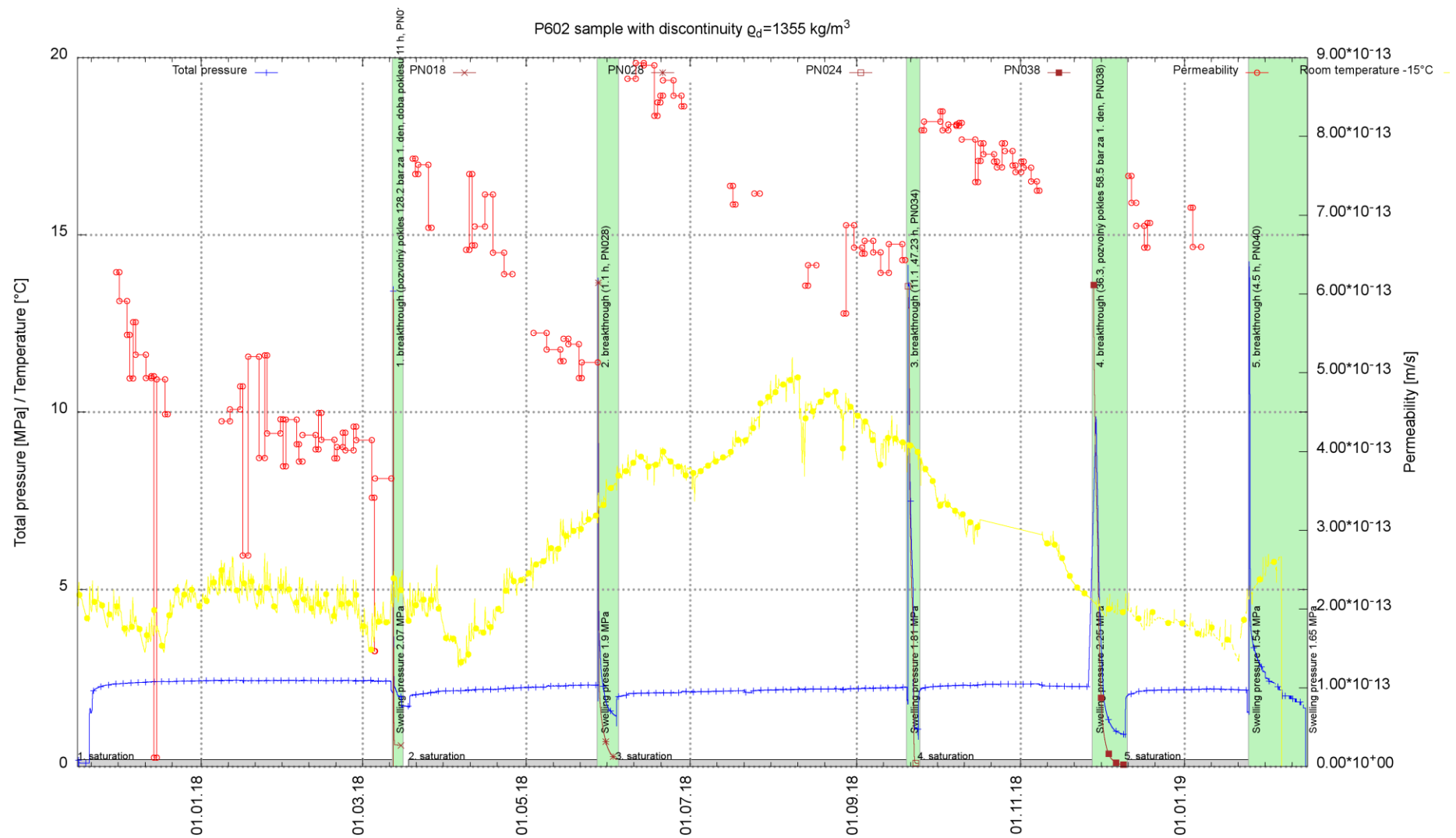


Fig. 19 Sample P602 (summary)

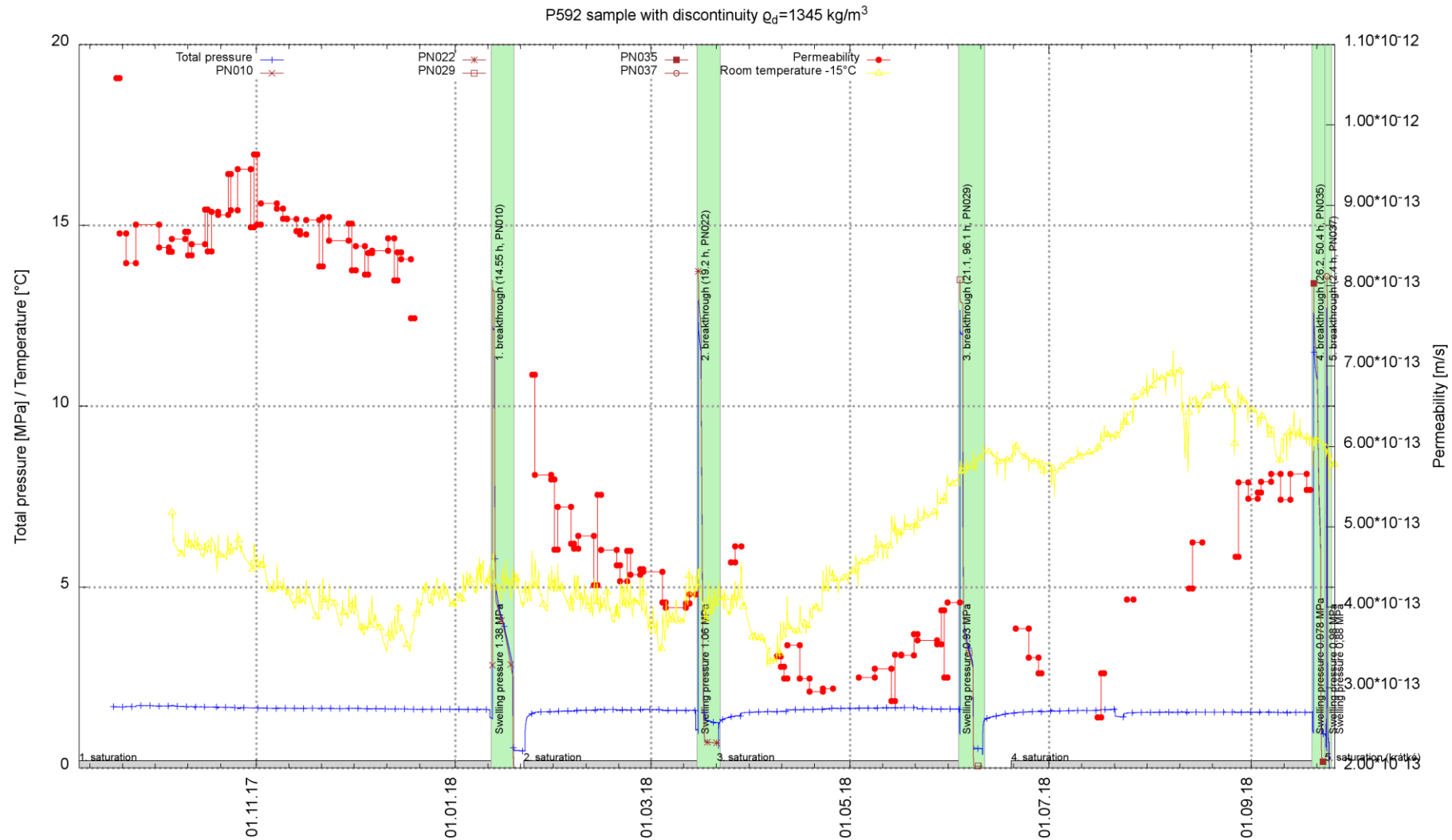


Fig. 20 Sample P592 (summary)

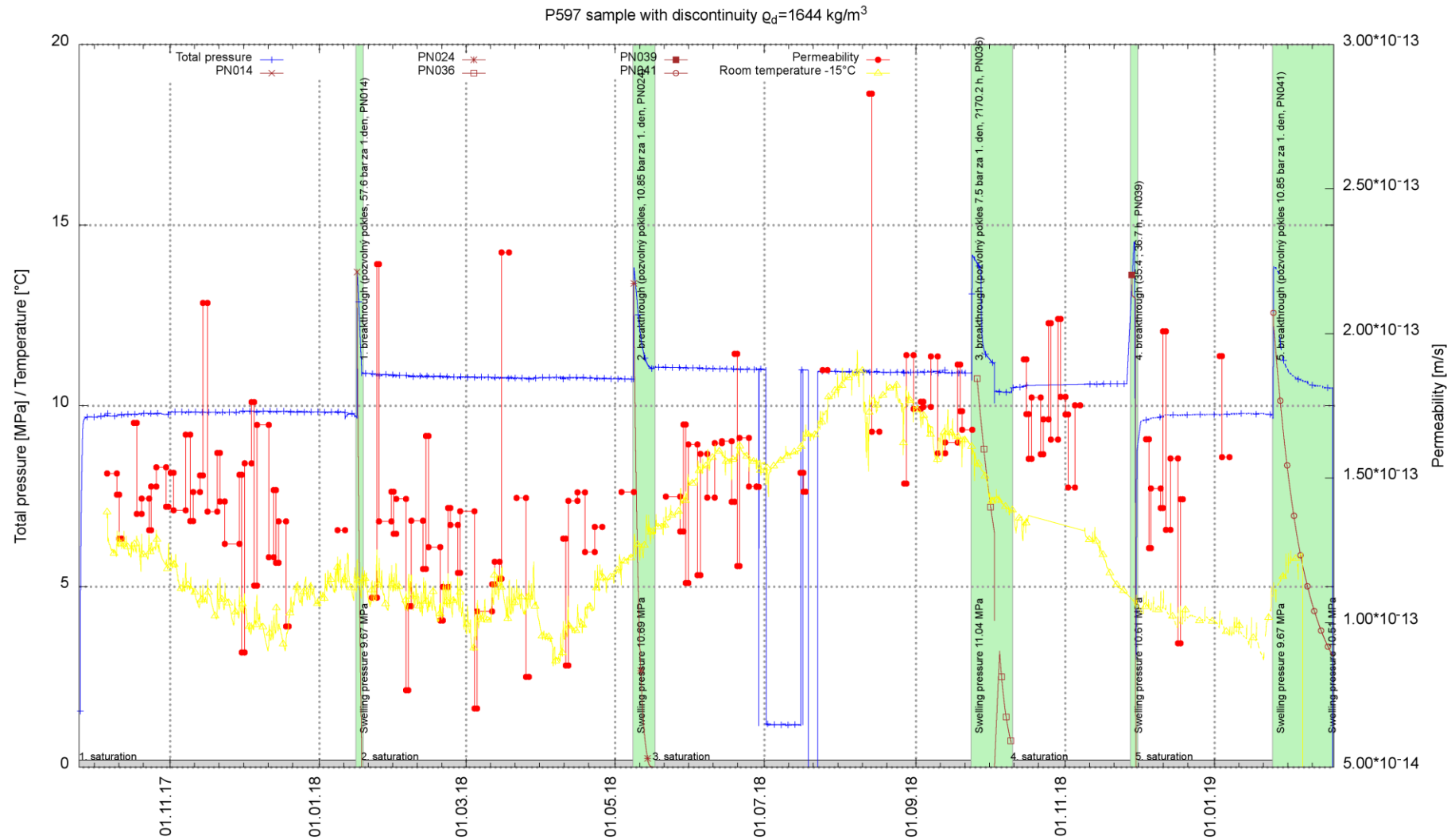


Fig. 21 Sample P597 (summary)

3.4 Evaluation of the results

The fourth stage of the research consisted of the repetition of the loading of the samples of saturated bentonite with air at high pressure (~12 MPa) and the experimental investigation of the breakthrough dynamics dependent on the swelling pressure (bulk density) of the material and, in particular, of whether self-healing occurs and whether the self-healing ability deteriorates following the repeated testing of the material (increased permeability, reduced breakthrough time).

The tests were conducted on 5 homogeneous samples and 3 samples with discontinuities. The dry density of the samples was between 1165 and 1744 kg/m³. A total of 30 saturation-breakthrough cycles was performed.

Summary results for the homogeneous samples are provided in Tab. 3 and Fig. 14 - Fig. 18.

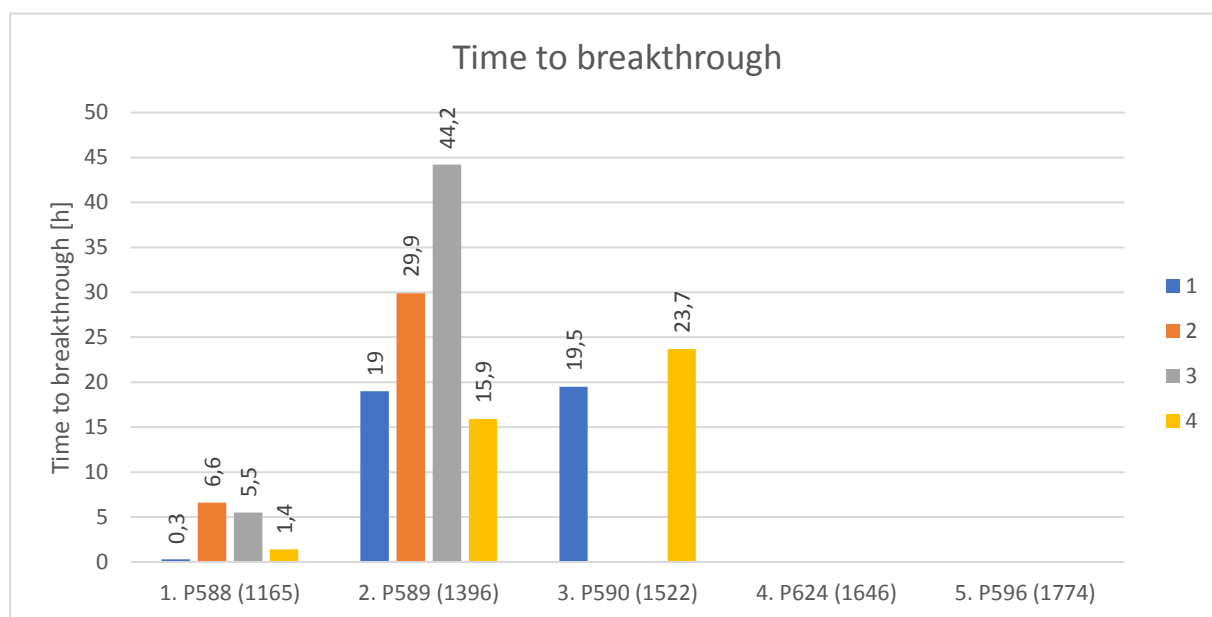


Fig. 22 Time to breakthrough for the homogeneous samples (the longer the time, the better the result; the number in the legend indicates the loading cycle)

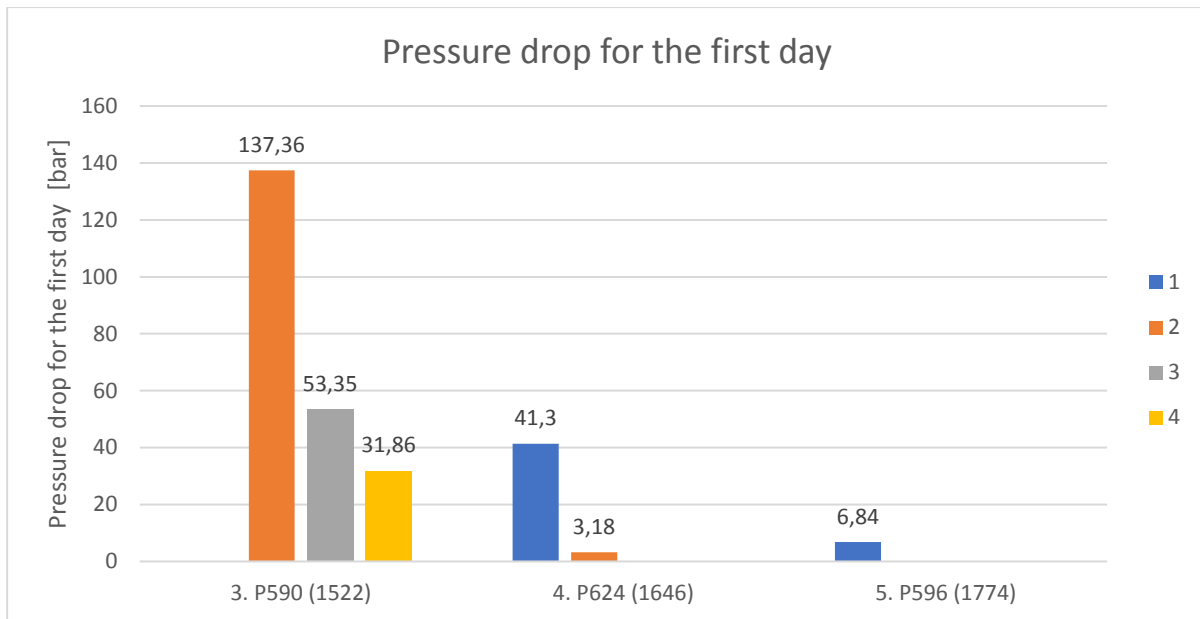


Fig. 23 Pressure drop for the first day for the homogeneous samples (the lower the value, the better the result; the number in the legend indicates the loading cycle)

Fig. 22 - Fig. 25 provide comparisons of the cycles for each of the samples (each cycle is shown in a different colour) and Fig. 22 and Fig. 23 provide comparisons of the results of the breakthrough tests. In the event that breakthrough was attained (the samples with lower bulk densities), the time required to achieve breakthrough is shown in Fig. 22. With concern to those cases where breakthrough was not attained and/or there was a gradual decrease in pressure with no significant failure, the results are shown in Fig. 23. A decrease always occurred on the first day of the test. Although the results vary, they do not indicate the degradation of the samples; on the contrary, most of the samples demonstrated a gradual improvement in the properties of the material. Even with respect to the sample with a higher bulk density (P624), no breakthrough was evident in the later stages.

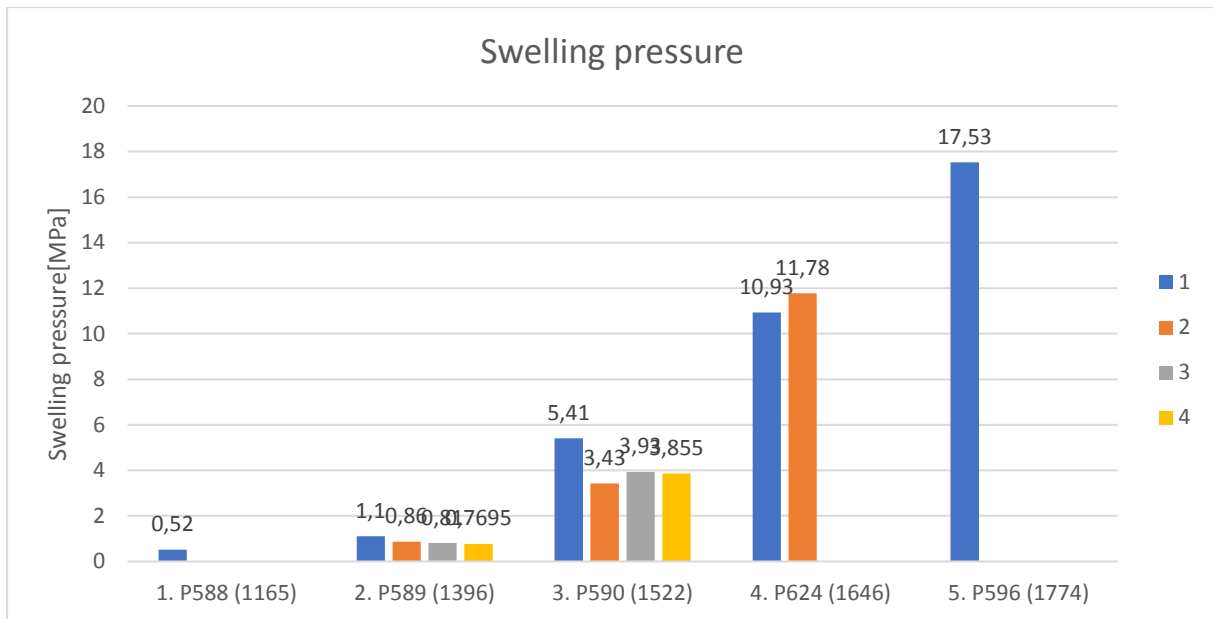


Fig. 24 Swelling pressure at the end of the saturation phase for the homogeneous samples (the higher the value, the better the result; the number in the legend indicates the loading cycle)

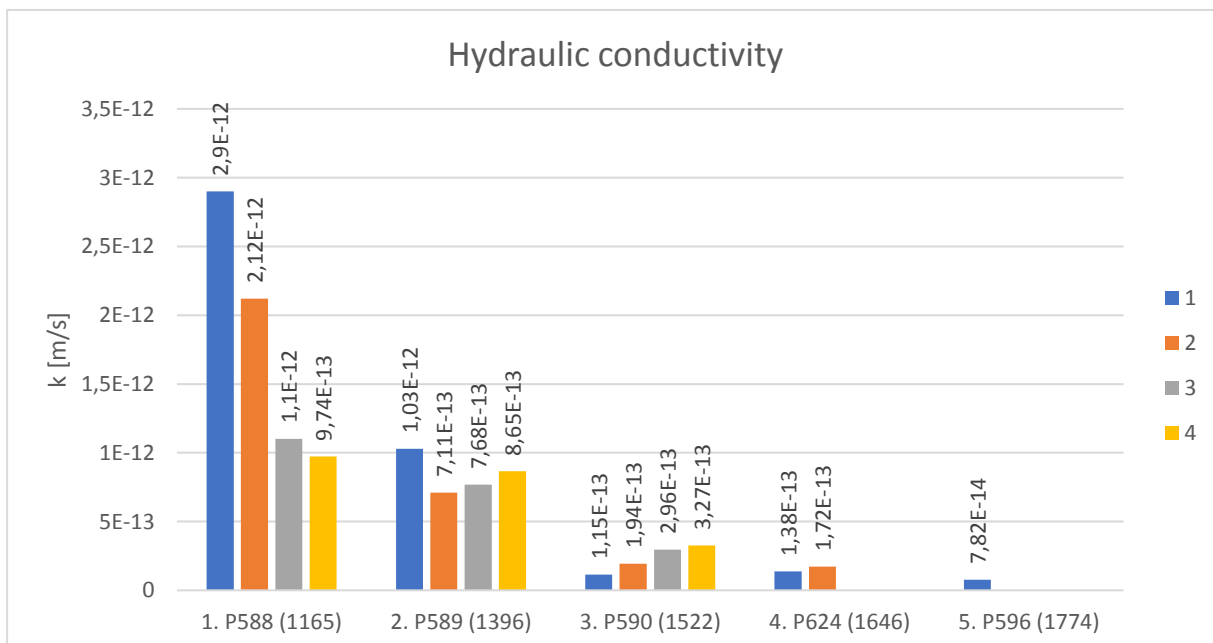


Fig. 25 Hydraulic conductivity at the end of the saturation phase for the homogeneous samples (the lower the value, the better the result; the number in the legend indicates the loading cycle)

Fig. 24 and Fig. 25 provide a comparison of the hydraulic conductivity and swelling pressure results at the end of the saturation phase and prior to the breakthrough tests. Thus, the first value refers to the “undamaged” sample.

The swelling pressure values (Fig. 24) exhibited a slight decrease concerning two samples (P589, P590) following the first breakthrough; the decrease later stabilised with no further continuation of the decreasing trend. Sample P588 most likely followed a similar trend;

however, due to the pre-stressing of the sample/sensor in the pressure tests, no exact values are available. In contrast, sample P624 exhibited an increase in swelling pressure.

The hydraulic conductivity values of sample P588 exhibited a gradual decrease, whereas with respect to the other samples, an initial decrease was evident followed by a slow gradual increase. It is not possible to state from the shape of the decrease/increase curve whether stabilisation or further changes occurred following subsequent breakthroughs. However, it is considered unlikely that any order changes occurred with concern to the hydraulic conductivity.

Summary results for the samples with discontinuities are provided in Tab. 4 and Fig. 19 - Fig. 21.

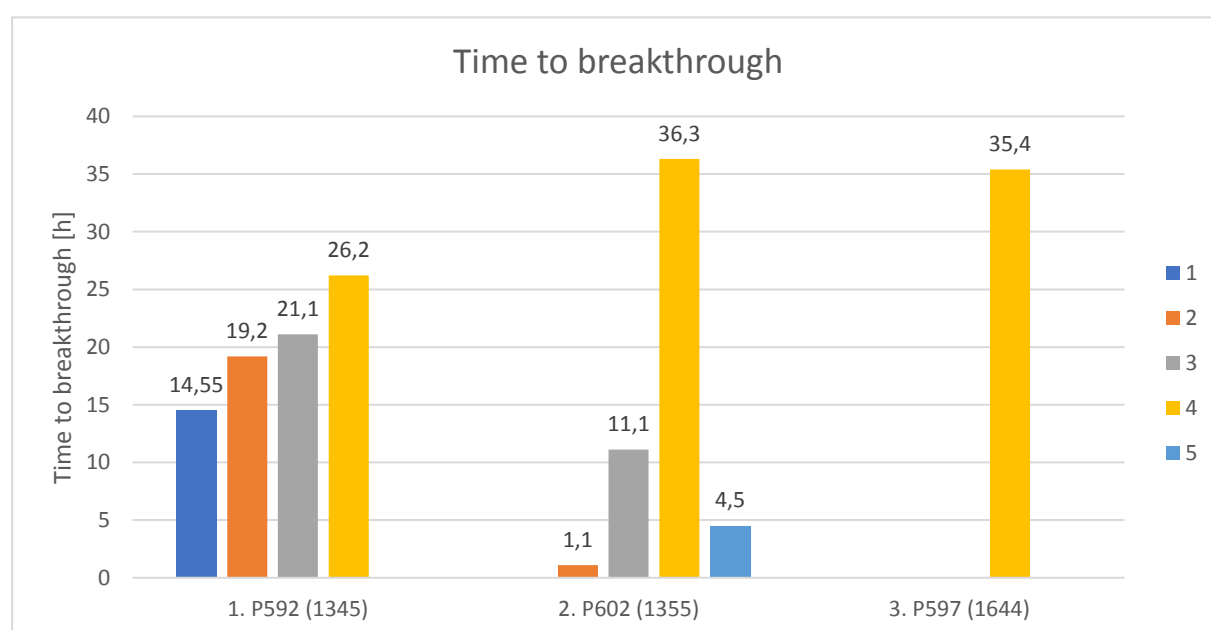


Fig. 26 Time to breakthrough for the non-homogeneous samples (the higher the value, the better the result; the number in the legend indicates the loading cycle)

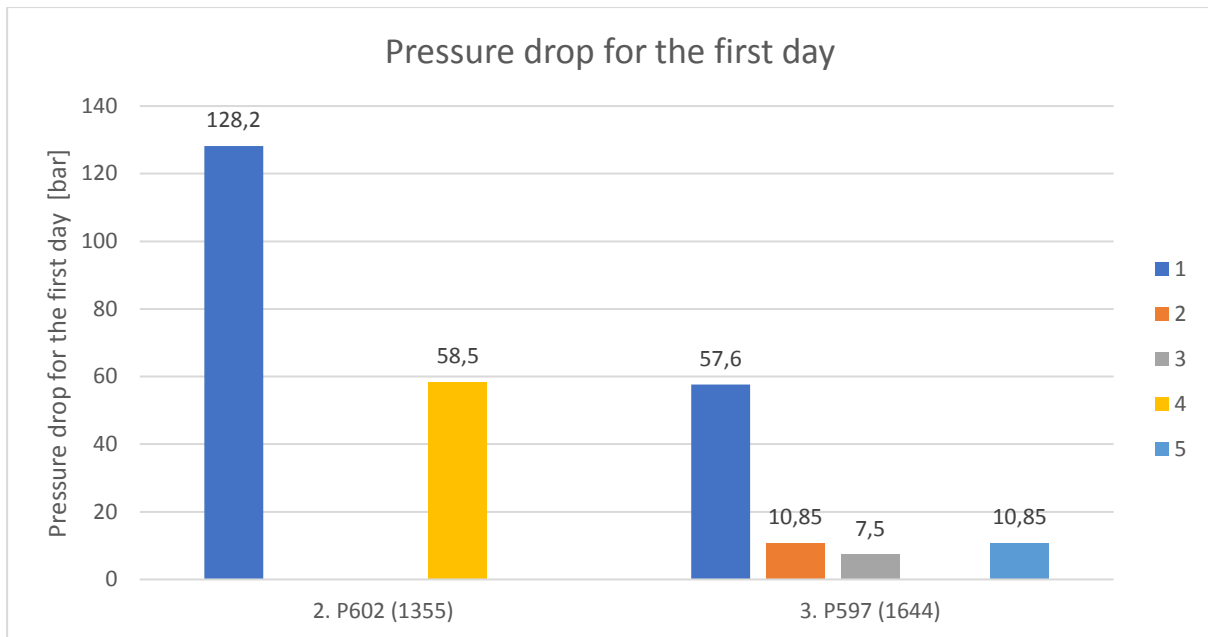


Fig. 27 Decrease in pressure for the first day for the inhomogeneous samples (the lower the value, the better the result; the number in the legend indicates the loading cycle)

Fig. 26 - Fig. 29 provide a comparison of the cycles of each of the samples with discontinuities (each cycle is shown in a different colour) and Fig. 26 and Fig. 27 provide comparisons of the results of the breakthrough tests. In the event that breakthrough was attained (the samples with lower bulk densities), the time required to achieve breakthrough is shown in Fig. 26. With concern to those cases where breakthrough was not attained and/or there was a gradual decrease in pressure with no significant failure, the results are shown in Fig. 27. A decrease always occurred on the first day of the test. Although the results vary, they do not indicate the degradation of the samples; on the contrary, most of the samples demonstrated a gradual improvement in the properties of the material. Even with respect to the sample with a higher bulk density (P597), no breakthrough was evident in the later stages.

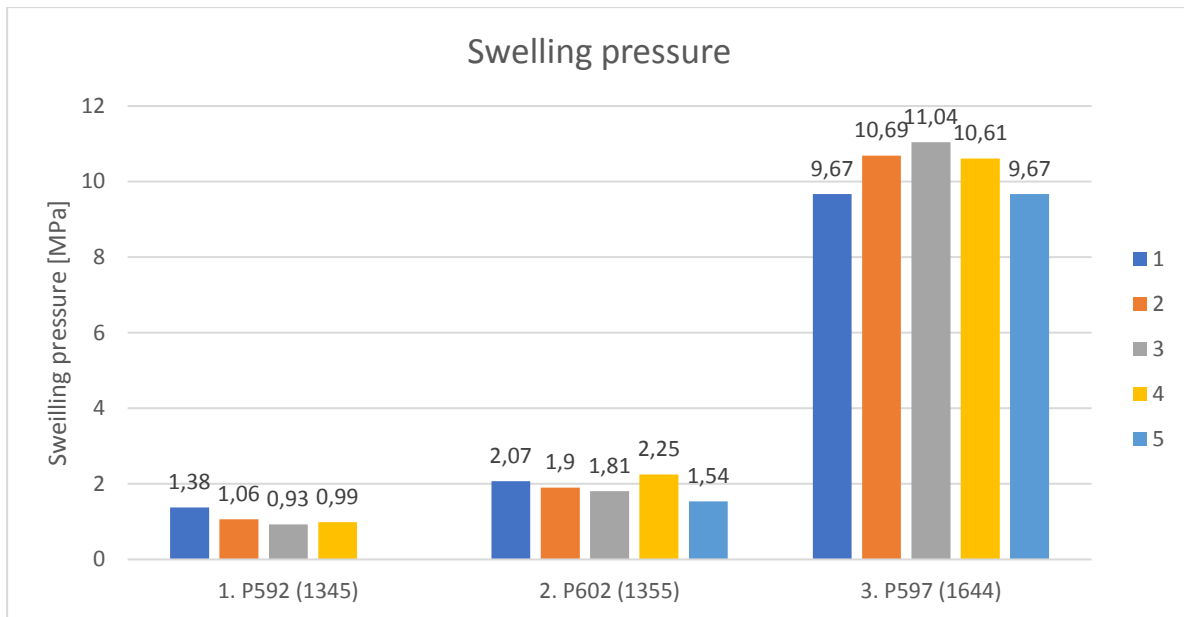


Fig. 28 Swelling pressure at the end of the saturation phase for the non-homogeneous samples (the higher the value, the better the result; the number in the legend indicates the loading cycle)

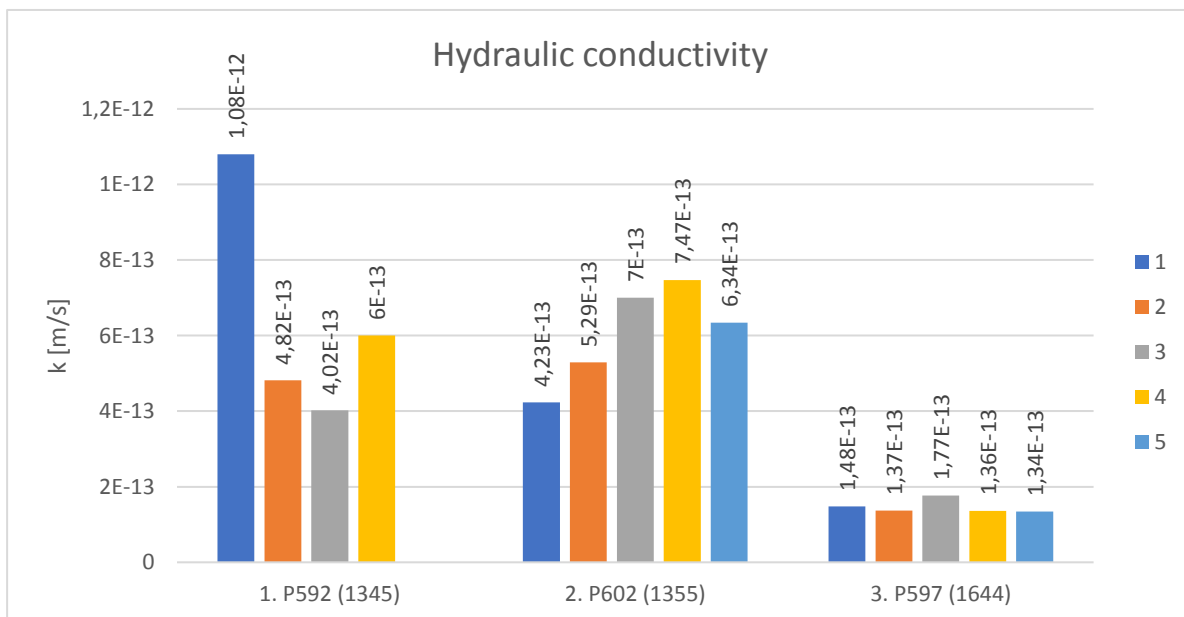


Fig. 29 Hydraulic conductivity at the end of the saturation phase for the non-homogeneous samples (the lower the value, the better the result; the number in the legend indicates the loading cycle)

Fig. 28 and Fig. 29 provide a comparison of the hydraulic conductivity and swelling pressure results at the end of the saturation phase and prior to the breakthrough tests. Thus, the first value refers to the “undamaged” sample.

The swelling pressure values (Fig. 28) exhibit a very slight decrease with concern to two samples (P592, P602) following the first breakthrough; the decrease later stabilised with no further continuation of the decreasing trend or, conversely, the pressure in a number of cycles increased slightly. The variation in the values was, however, minimal. Concerning sample

P597, the swelling pressure increased gradually and subsequently returned to the default value.

The hydraulic conductivity values (Fig. 29) initially exhibited a decrease with respect to sample P592, followed by a slight increase. Conversely, sample P602 exhibited an initial value increase followed by a decrease. The finally attained values for samples P592 and P602 were similar (the samples had a similar bulk density; however, sample P592 exhibited a higher degree of inhomogeneity, which was probably the reason for the more significant changes). Sample P597 exhibited a slight oscillation around the original values.

It is not possible to determine a fully qualified conclusion from the shape of the decrease/increase curve; however, the values and variability of the changes indicate the probable occurrence of stabilisation in the absence of any significant (order) changes.

The character of the results for the homogeneous and, particularly, the inhomogeneous samples suggests that in addition to the gas permeability tests themselves, the time-scale also exerted a significant influence. In order to form a comprehensive assessment of the various tests, Fig. 30 and Fig. 31 provide a comparison of the swelling pressure and permeability of the homogeneous and non-homogeneous samples dependent on bulk density versus the results of the reference (short term) test results (Hausmannová 2018).

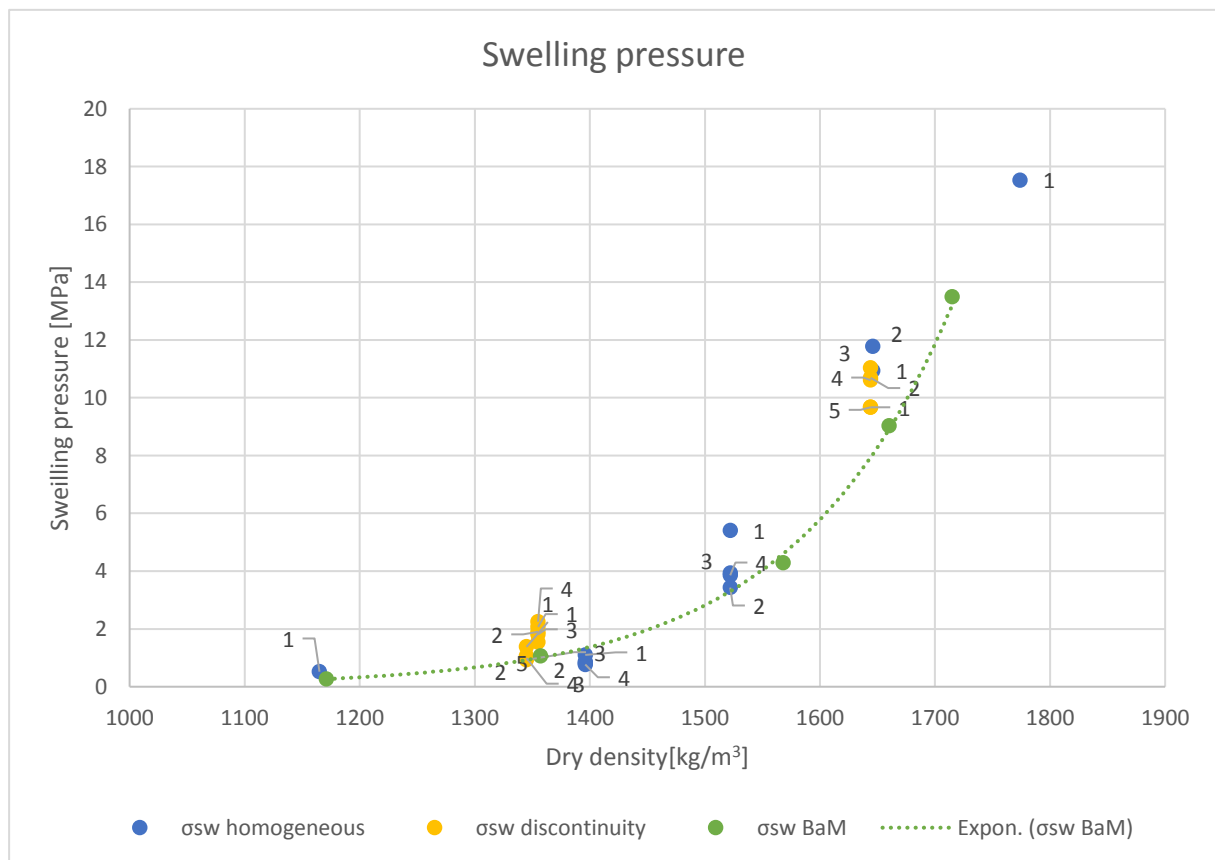


Fig. 30 Swelling pressure dependent on dry density (the number near the point indicates the loading cycle)

The results show (Fig. 30) that in comparison to the reference values the gas permeability tests did not exert a negative effect on swelling pressure; indeed, most of the values are higher than the reference values. However it is necessary here to consider the time aspect, i.e. it is clear that the processes at work in the BaM material are long-term. Thus, a more accurate comparison would require the consideration of values for intact samples that had been saturated over the same time period. The comparison of the samples with and without discontinuities does not indicate any fundamental effect exerted by the discontinuities, i.e. after a sufficient time period, the samples were seen to behave in a similar manner.

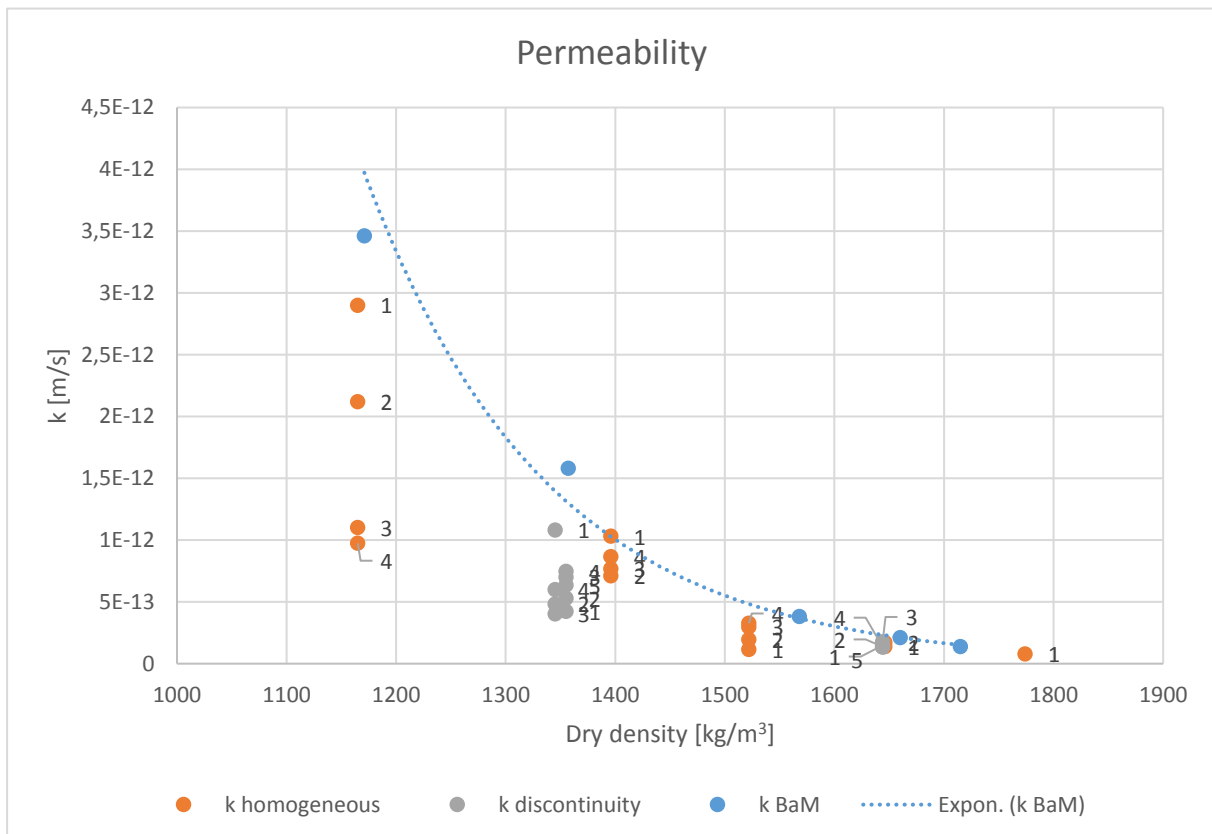



Fig. 31 Hydraulic conductivity dependent on dry density (the number near the point indicates the loading cycle)

The hydraulic conductivity results (Fig. 31) are similar to those from the comparison of swelling pressure. The breakthrough results are lower than the reference values, the time scale is of significant importance and no clear difference is evident between the samples with and without discontinuities.

A comparison of the gas permeability tests for the homogeneous and inhomogeneous samples dependent on dry density is provided in Fig. 32 and Fig. 33. Fig. 32 shows the breakthrough time, while Fig. 33 shows the drop in the injection pressure for the first day for those samples where the breakthrough time could not be determined. With the exception of the higher proportion of samples with discontinuities in the group that exhibited a gradual decrease in pressure, no significant differences were observed. Indeed, it is clear that there was an overall dependence on the dry density of the samples.

 SÚRAO	<i>Experimental assessment of the gas permeability of engineered barriers in a deep geological repository – final report</i>	Evidenční označení:
		SÚRAO TZ 384/2019/ENG

Note: The results with very low values in Fig. 33 (near the bottom of the graph) probably indicate that there was a leak in the system rather than the occurrence of breakthrough.

In addition to higher representation in the group in Fig. 29, the group of samples with discontinuities also contained a higher percentage of cases wherein the breakthrough tests were characterised by two pressure decreases. Moreover, it took a much longer time (= more cycles) for some of the specimens to begin to “seal” and for the formation of a breakthrough point. This would tend to indicate that although the permeability and swelling pressure were more or less stable, the discontinuities had not fully “healed”.

Note: Following the dismantling of the samples, it was not evident that the discontinuities (still apparent) provided the only breakthrough path, i.e. a network of paths was observed on most of the samples.

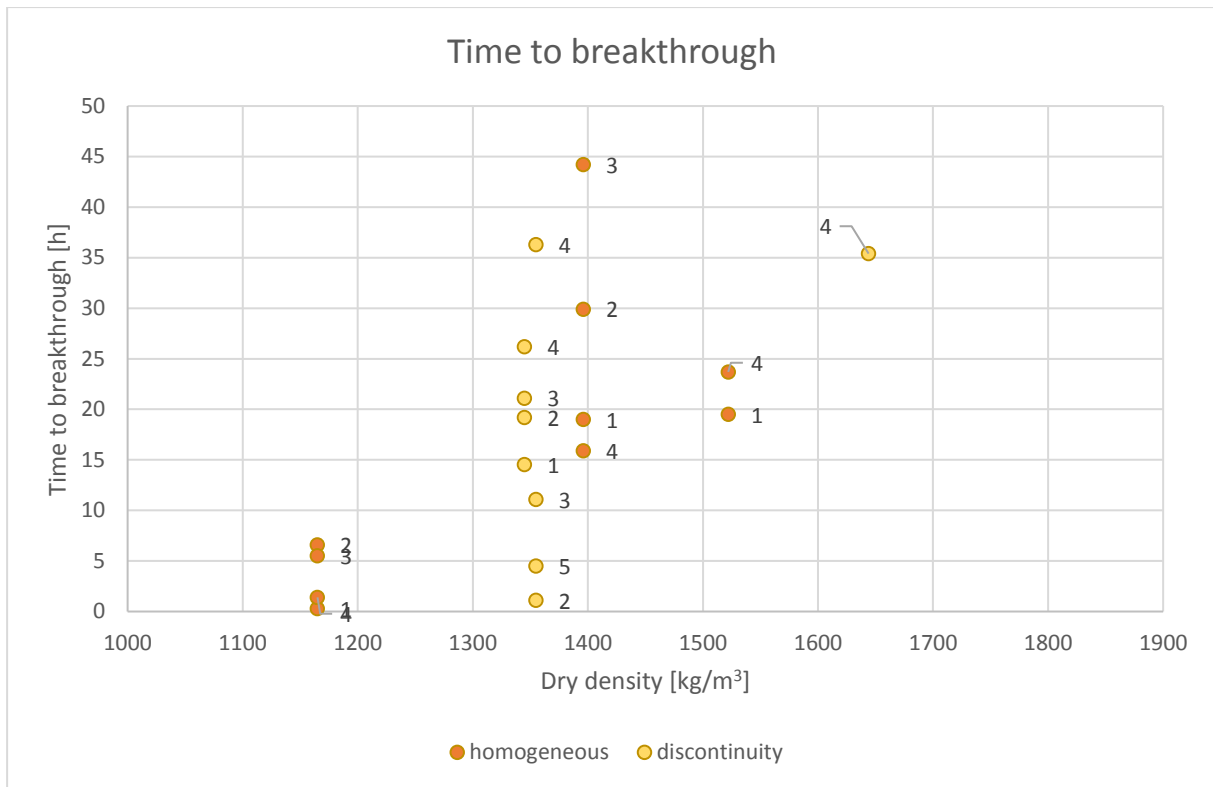


Fig. 32 Breakthrough time (the number near the point indicates the loading cycle)

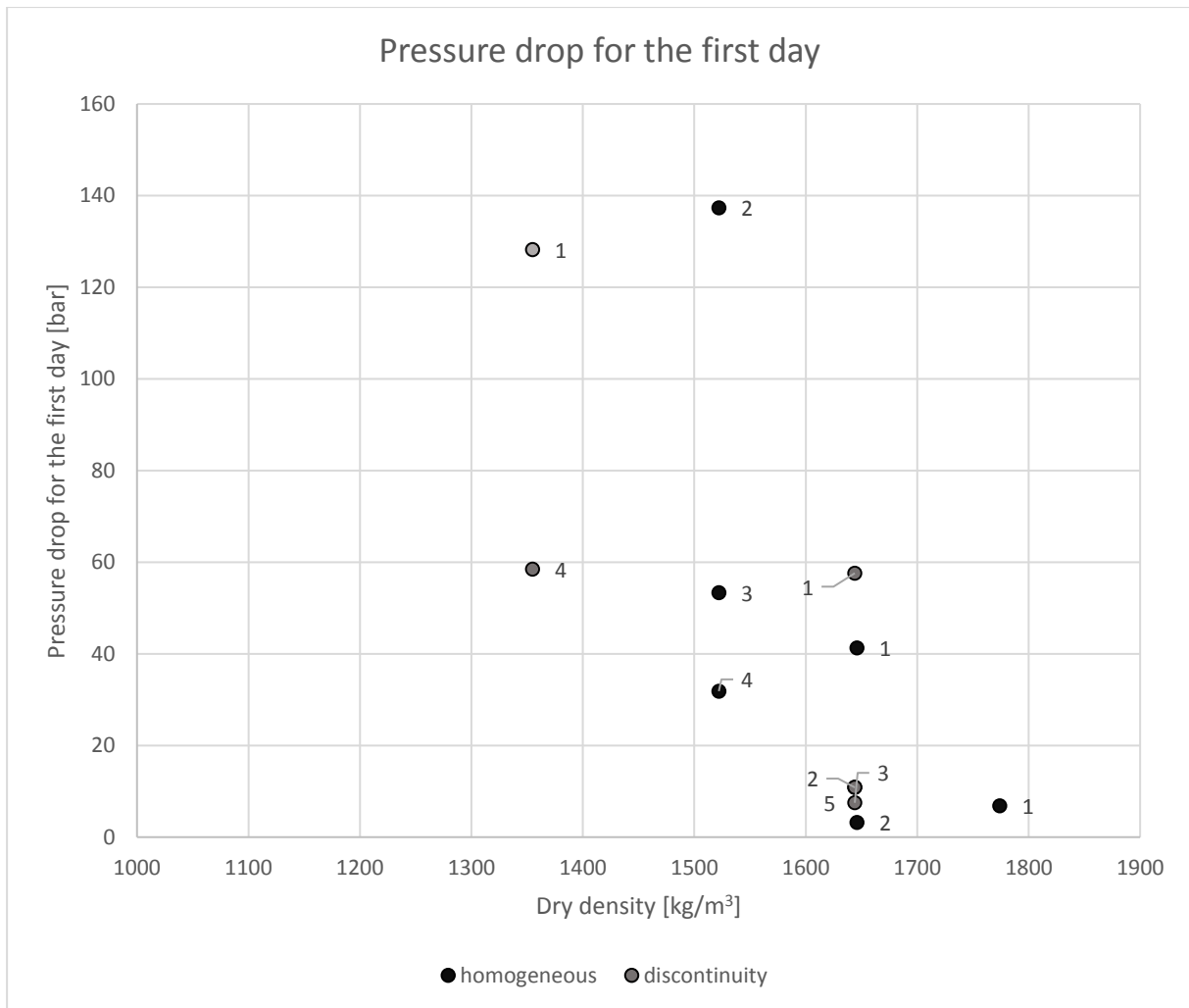



Fig. 33 Pressure drop at day 1 (the number near the point indicates the loading cycle)

 SÚRAO	<i>Experimental assessment of the gas permeability of engineered barriers in a deep geological repository – final report</i>	Evidenční označení:
		SÚRAO TZ 384/2019/ENG

4 Conclusion

The fourth stage of the research consisted of the initial experimental analysis of the BaM engineered barrier material with concern to gas permeability and its self-healing ability.

The research was divided into two main areas:

- a. The gas permeability of bentonite with natural water content
- b. The gas permeability of saturated bentonite – cyclical breakthrough and saturation tests

The results obtained from both research areas clearly showed that the main determinant of the behaviour of BaM material in terms of gas permeability consists of its dry density, i.e. the properties of BaM improve with increases in this parameter.

The results obtained from the second research area did not indicate the gradual degradation of the material due to the cyclical performance of gas tests. While in some cases there was a deterioration in the material properties, the process soon stabilised and was not significant. In fact, the hydraulic conductivity and swelling pressure values were, in most cases, observed to be systematically better than the reference values for this material.


The results indicated the significant impact of the time factor, i.e. long-term saturation exerted a significant impact on the properties of the BaM material.

The influence of the time scale was particularly evident concerning the samples with discontinuities. Although the permeability and swelling pressure values did not change significantly over time, the breakthrough value stabilisation process lasted significantly longer than it did for the homogeneous samples; moreover, the behaviour of the two types of samples differed during the test procedure.


The findings from this research stage indicated that:

- Processes at work within the material are long term and need to be investigated from the long-term perspective
- The stabilisation of permeability and swelling pressure values cannot be taken as indicators of the termination of mechanical changes within the bentonite (homogenisation). These values stabilise significantly earlier than the initiation of self-healing.
- While gas breakthrough does not lead to the destruction of the material, its sealing function in the engineered barrier may be slightly negatively affected. The function of the material is restored following re-saturation.
- Discontinuities do not pose a threat to the functioning of the engineered barriers. An important factor concerns the average dry density after taking into account the free space and a saturation time sufficient so as to attain homogenisation – the self-healing of discontinuities. Hence, the engineered barrier should be considered as a complex system that includes discontinuities, whether they be technological gaps or gaps caused by the composition of the material (gaps between bentonite pellets).

The gas permeability tests performed at this stage of the research should be considered to be introductory. The research revealed the significance both of the non-deterministic behaviour

 SÚRAO	<i>Experimental assessment of the gas permeability of engineered barriers in a deep geological repository – final report</i>	Evidenční označení:
		SÚRAO TZ 384/2019/ENG

of the material in the breakthrough tests and the need for a long-term testing programme. The testing of the non-homogeneous material addressed only a simple longitudinal discontinuity, whereas under real repository conditions, the barrier will feature a whole network of such discontinuities. Therefore, the gradual upscaling of the issue will be required involving the conducting of complex and comprehensive testing. Moreover, since the experimental analysis did not address materials that are inhomogeneous as a result of their form (i.e. pellets), the behaviour of such materials will also need to be verified in the future.

 SÚRAO	<i>Experimental assessment of the gas permeability of engineered barriers in a deep geological repository – final report</i>	Evidenční označení:
		SÚRAO TZ 384/2019/ENG

5 Literature

Hausmannová, L., Hanusová, I., Dohnálková, M. (2018) Shrnutí výzkumu českých bentonitů pro hlubinné úložiště - do roku 2018, SÚRAO TZ 309/2018

ČVUT CEG (2017) Interní postup č. 182/28 Stanovení plynopropustnosti nenasycených zemin.

OUR SAFE FUTURE



SÚRAO

Radioactive Waste Repository Authority
Dlážděná 6, 110 00 Prague 1, Czech Republic
Tel.: +420 221 421 511, E-mail: info@surao.cz
www.surao.cz